

**TH-AM-1 FLUORIMETRIC STUDIES OF F-ACTIN LABELED WITH DANSYL AZIRIDINE.** T.-I. Lin, Cardiovascular Research Institute, University of Calif., San Francisco, CA 94143

A fluorescent probe, dansyl aziridine, has been specifically attached to the 373-cys of F-actin. The probe attached to actin exhibits a 65 nm blue shift of its emission maximum and a 5-fold fluorescence enhancement indicating that it is located in a hydrophobic environment. Excitation spectrum of the protein adduct shows energy transfer from aromatic residues to the dye. The modification does not impair the G-F transformation of actin, nor does it affect the complex formation of actin and myosin as judged by viscosity measurements and superprecipitation. However labeled actin stimulates the  $Mg^{2+}$ -ATPase of myosin only about 75% as well as unmodified actin. The fluorescence of the actin adduct is enhanced by the addition of EDTA, ATP and pyrophosphate.  $Mg^{2+}$  antagonizes this effect reversibly. However in the presence of 10 mM phosphate buffer (pH 7.4) these effects disappear. The results are in accord with the recent finding by Nonomura *et al.* [*J. of Biochem.* 78 1101 (1975)] viz., the filament structure of F-actin is strengthened by orthophosphate. The association of labeled F-actin with myosin subfragment-1 (s-1) and heavy meromyosin (HMM) have been monitored by the enhancement of the emission maximum at 495 nm (excite at 350 nm). Titration of 0.5  $\mu M$  actin in 0.15 M KCl, 10mM phosphate (pH 7.4) at 25°C throughout a wide range of concentration of S-1 reveals 1:1 association curve. The titration curve of actin with HMM shows 2:1 association and positive cooperativity indicating that the binding of first head of HMM facilitates the binding of second head. Supported by grants NSF PCM 75-22698, NHLBI HL-16683, and AHA 60-CI-08.

**TH-AM-2 EVIDENCE THAT THE  $Ca^{2+}$  ACTIVATION OF SOLEUS AND CARDIAC MUSCLE IN THE RABBIT IS CONTROLLED BY PROTEINS OTHER THAN, OR IN ADDITION TO TROPONIN.** W.G.L. Kerrick, D.A. Malenick,\* P.E. Hoar, R. Coby,\* and E.H. Fischer.\* Department of Physiology and Biophysics and Department of Biochemistry, University of Washington, Seattle, Washington 98195.

Comparisons were made between the  $Ca^{2+}$  and  $Sr^{2+}$  activated tension and actomyosin ATPase in rabbit skinned skeletal and cardiac muscle fibers, as well as in a reconstituted troponin, tropomyosin, actin, and myosin system. The  $Ca^{2+}$  and  $Sr^{2+}$  activated tensions and ATPase activities of white muscle correlated well with each other. The  $Sr^{2+}$  concentration required for half maximum activation for both tension and ATPase was 7 times higher than for  $Ca^{2+}$ . In contrast, the concentration of  $Ca^{2+}$  and  $Sr^{2+}$  required to activate tension in skinned soleus (slow twitch) and cardiac muscle fibers was essentially the same.  $Ca^{2+}$  and  $Sr^{2+}$  activation of actomyosin ATPase from desensitized skeletal muscle myofibrils in the presence of cardiac troponin has been shown to be 3-7 times more sensitive to  $Ca^{2+}$  than  $Sr^{2+}$ . These data, in conjunction with the known divalent cation selectivity of  $Ca^{2+}$  binding proteins such as troponin, TNC, parvalbumin, and myosin light chains, suggest the possibility that other controlling factors might be involved in the  $Ca^{2+}$  control of soleus and cardiac muscle, aside from  $Ca^{2+}$  binding to troponin. The incorporation of phosphate from  $\gamma$  labeled ATP<sup>32</sup> into these skinned fibers was determined under the same conditions used for tension and ATPase measurements. Phosphate was incorporated into the 19,000 MW myosin light chain, TNT, and higher molecular weight proteins in skinned soleus and cardiac fibers in contrast to white fibers where no phosphorylation could be observed. These results suggest that phosphorylation reactions could play a crucial role in the  $Ca^{2+}$  activation of soleus and heart muscle. Supported by PHS NS05082 and AM17081, The Muscular Dystrophy Association, and the American Heart Association.

**TH-AM-3 CHARACTERIZATION OF THE MAJOR CONTRACTILE PROTEINS OF SKINNED SKELETAL AND CARDIAC MUSCLE FIBERS WITH SDS GELS.** P.E. Hoar, D.A. Malenick,\* and W.G.L. Kerrick, Department of Physiology and Biophysics and Department of Biochemistry, University of Washington, Seattle, Washington 98195.

It has been previously shown that the  $Ca^{2+}$  activation of skinned fibers varies with the species and the type of muscle. Although many purified muscle proteins have been characterized, little is known about their stoichiometry and comparative role in the  $Ca^{2+}$  activation of muscle (particularly slow twitch and cardiac). The purpose of this study was to determine the stoichiometry and molecular weights of the major contractile and regulatory proteins present in skinned fibers of different muscle types. Mechanically disrupted (functionally skinned) fibers identical to those used for tension measurements were dissolved in a sample buffer containing SDS and subjected to polyacrylamide gel electrophoresis. Gels were stained with Coomassie Brilliant Blue, and scanned in a densitometer at 570 nm. Using purified proteins as calibration standards, the following approximate molar ratios were found in fibers from the rabbit adductor magnus (a white muscle): actin: TNT: tropomyosin: TNI: TNC: myosin: myosin light chains equal to 7: 1: 1: 1: 1: 4 respectively, in agreement with results previously reported for rabbit myofibrils (Potter, J.D., *Arch. Biochem. Biophys.*, 162, 436 (1974)). By comparison, there appeared to be less TNC in slow twitch soleus fibers. The actin bands of soleus and cardiac muscle showed less protein relative to the same band in white muscle. Also, the myosin heavy to light chain ratio in cardiac muscle was higher than in skeletal muscle fibers.

Supported by PHS AM17081 and NS05082, The Muscular Dystrophy Association, and The American Heart Association.

TH-AM-4 <sup>19</sup>F-NMR STUDIES OF CALCIUM INDUCED CHANGES IN TROPONIN. L.H. Strong,\* E.T. Fossel\* and J. Gergely, Dept. Muscle Research, Boston Biomedical Research Institute; Dept. Neurol., Massachusetts Gen. Hospital; and Dept. Biol. Chem., Harvard Med. School, Boston, Mass. 02114

Troponin-C (TnC) labeled at Cys 98 with 3-bromo-1,1,1-trifluoropropanone (TFP) shows a well resolved <sup>19</sup>F NMR resonance whose amplitude diminishes by the addition of Ca<sup>2+</sup>. Two mol of Ca<sup>2+</sup>/mol of TnC are required to completely eliminate the <sup>19</sup>F signal. This indicates that upon saturation of the two Ca<sup>2+</sup>-Mg<sup>2+</sup>-sites of TnC (Potter and Gergely, J. Biol. Chem. 250,5681,1975) the environment of the probe changes so as to immobilize the F-atoms. To investigate the effect of Ca<sup>2+</sup> binding to TnC on the TnI component of Tn, TnI labeled with TFP was complexed with native TnC or with TnC containing a maleimide spin label at Cys 98. With unmodified TnC the F-spectra show two overlapping lines; adding Ca<sup>2+</sup> produces a shift in the relative intensity. The changes are again essentially complete upon addition of 2 mol Ca<sup>2+</sup>/mol of TnC. With spin labeled TnC the F-resonance of TnI is broader than with native TnC. Addition of Ca<sup>2+</sup> narrows the line, the effect being maximal at 2 mol/ml. These results show that TFP is a useful tool for the investigation of Ca<sup>2+</sup> induced changes in the troponin system. The fact that changes in the F-label in TnI occur on Ca-binding to both the native and spin labeled TnC indicates that Ca<sup>2+</sup>-induced conformational changes in TnC result both in a conformational change in TnI and in a change in distance between the F-probe and the spin label. It is of interest that the changes induced in TnI by Ca<sup>2+</sup> binding to TnC reported by this probe are attributable to binding to the Ca<sup>2+</sup>-Mg<sup>2+</sup> sites, in contrast to a dansyl label attached to TnI, which responds to Ca<sup>2+</sup> binding to the Ca<sup>2+</sup>-specific sites of TnC (Leavis, Fed. Proc. 35,1746,1976). (Supported by grants from NIH, NSF, MDAA and a fellowship (E.T.F.) of the Arthritis Foundation)

TH-AM-5 NMR SPECTRAL CHARACTERISTICS OF CATION DEPENDENT CONFORMATIONS OF TROPONIN-C K. B. Seamon\*, D. J. Hartshorne\*, and A. A. Bothner-By\* (INTR. by R. Kay) Depts. of Chemistry and Biological Sciences, Carnegie-Mellon University, Pittsburgh, PA 15213

We have described the qualitative change in the 250 Mhz proton spectrum of rabbit skeletal troponin-C (TN-C) upon binding of Ca<sup>2+</sup> to the high affinity and low affinity metal binding sites. (Fed. Proc., 35 (7): 1363, 1976). The assignment of resonances to the tyrosine ring protons previously reported has been confirmed by the spectra of an iodinated derivative of TN-C in which both tyrosines are modified. It is shown that two spectral parameters are related linearly to the amount of Ca<sup>2+</sup> bound at the low affinity site. These are 1) the chemical shift of an upfield shifted methyl peak and 2) the chemical shift of an upfield shifted phenylalanine peak. The effect of Mg<sup>2+</sup> on the spectrum of the Ca<sup>2+</sup> free protein was studied. It is shown that the spectral changes observed on Mg<sup>2+</sup> binding are those associated with binding at the high affinity sites only. Cd<sup>2+</sup> is able to elicit the spectral changes characteristic of low affinity binding. A fluorinated derivative of TN-C was made by reacting the protein with bromotrifluoroacetone, a sulfhydryl specific alkylating reagent. The fluorine resonance shifts downfield upon adding Ca<sup>2+</sup> to the metal free protein. The same shift is effected when Mg<sup>2+</sup> is added to the metal free protein. This suggests that the fluorine probe is only sensitive to conformational changes induced by binding of metal at the high affinity site.

(Supported in part by NIH Grant #RR00292)

TH-AM-6 THE Ca<sup>2+</sup> BINDING PROPERTIES OF BOVINE CARDIAC TROPONIN-C. J.D. Potter, Department of Cell Biophysics, Baylor College of Medicine, Houston, TX 77030

Troponin-C from bovine cardiac muscle (C-TnC) has been purified to homogeneity. The amino acid sequence of C-TnC has recently been determined and compared to that of skeletal TnC (S-TnC) (van Eerd and Takahashi, Biochemistry 15:1171, 1976). It has been predicted that C-TnC contains only 3 Ca<sup>2+</sup> binding sites, in contrast to the 4 in S-TnC, and that the missing Ca<sup>2+</sup> binding site is in a region homologous to region I of S-TnC (res.8-48). The 3 other cardiac sites are thought to be similar to those in S-TnC. Previous work has shown that S-TnC contains two high affinity (K<sub>Ca</sub>=2.1x10<sup>7</sup>M<sup>-1</sup>) Ca<sup>2+</sup> binding sites that bind Mg<sup>2+</sup> competitively (Ca<sup>2+</sup>-Mg<sup>2+</sup> sites), and two Ca<sup>2+</sup> binding sites of lower affinity (K<sub>Ca</sub>=3.2x10<sup>5</sup>M<sup>-1</sup>) that do not bind Mg<sup>2+</sup> (Ca<sup>2+</sup>-specific sites) (Potter and Gergely, J. Biol. Chem. 250:4628, 1975). It was of interest, therefore, to do a detailed Ca<sup>2+</sup>-binding study of C-TnC to determine the nature of the putative missing site. The Ca<sup>2+</sup> binding results reported here show that there are two sites which have a high affinity for Ca<sup>2+</sup> (K<sub>Ca</sub>≈10<sup>7</sup>M<sup>-1</sup>), and that the affinity of these sites for Ca<sup>2+</sup> is reduced in the presence of 2 mM MgCl<sub>2</sub> (K<sub>Ca</sub>≈2x10<sup>6</sup>M<sup>-1</sup>). The K<sub>Mg</sub> for these sites is calculated to be ~2x10<sup>3</sup>M<sup>-1</sup>. Thus, C-TnC contains two Ca<sup>2+</sup>-Mg<sup>2+</sup> sites very similar to those in S-TnC. Preliminary results suggest that C-TnC also contains one additional site of lower Ca<sup>2+</sup> affinity (K<sub>Ca</sub>≈10<sup>4</sup>M<sup>-1</sup>) which does not bind Mg<sup>2+</sup>. Although the Ca<sup>2+</sup>-affinity of this site is lower than in S-TnC, its properties are analogous to the Ca<sup>2+</sup>-specific sites of S-TnC. Based on the fact that C-TnC appears to lack a Ca<sup>2+</sup>-specific site and that region I is believed to have lost its ability to bind Ca<sup>2+</sup>, it is proposed that region I is the location of one of the Ca<sup>2+</sup>-specific sites in TnC. (Supported by grants from the AHA, the AHA, Tx. Affiliate and an Established Investigatorship of the AHA.)

**TH-AM-7 THE HIGH AFFINITY CALCIUM SITES OF TROPONIN-C DIRECT AND STABILIZE THE FOLDING OF ALMOST ALL OF THE STRUCTURE.** B.A. Levine† J. Thornton‡ D. Coffman‡ and D.A. Mercola, Inorganic Chemistry Laboratory and Department of Zoology, South Parks Road, Oxford, England.

Ca-saturated and Ca-free rabbit skeletal muscle troponin-C (TNC) has been studied by P.M.R. Ca-saturated TNC shows a spectrum indicative of a compact structure (1). Temperature dependence experiments to 95°C show a sharpening of resonances but very little or no change in chemical shift positions indicating that the structure is stable although increased mobility and breathing motions do occur. In contrast, Ca-free TNC shows less tertiary structure which is very nearly abolished upon heating to 65°C. We conclude that Ca ions direct and greatly stabilize the folding of TNC. Ca-titration experiments with Ca-free TNC show that there are two mutually exclusive sets of resonances, one undergoes chemical shifts with the titration of the first high affinity site (c.f. (2)) but is insensitive to subsequent sites and a second set which shift with titration of the second high affinity site but is insensitive to all other sites. These sets include assigned resonances of Lys, Tyr, Phe, Glu, and other methyl groups and so likely broadly sample both the interior and exterior of the protein. Therefore the two high affinity sites have different binding constants. After titration of the two high affinity sites the protein has acquired the heat stability of Ca-saturated TNC. Very few further shifts occur upon titration of the low affinity sites. We conclude that the protein folds in two distinct domains due to Ca binding to two separate sites and that binding at these sites stabilizes most of the structure. (1) B.A. Levine, D. A. Mercola, and J. Thornton, *Febs. Letts.*, 61, 218 (1976). (2) J. Potter and J. Gergely *J. Biol. Chem.*, 250, 4628 (1975).

**TH-AM-8 SPECTRAL STUDIES ON CALCIUM BINDING TO CARDIAC TROPONIN C.** Paul C. Leavis, Dept. Muscle Research, Boston Biomedical Research Institute, and Dept. Neurology, Harvard Medical School, Boston, Massachusetts, 02114

Bovine cardiac troponin C has been isolated by a procedure based on modifications of the methods of Tsukui and Ebashi (*J. Biochem.* 73:119, 1973) and Brekke and Greaser (*J. Biol. Chem.* 251:866, 1976). Ca<sup>2+</sup> titrations show a 45% enhancement of intrinsic (tyr) fluorescence and a 30% increase in the CD at 222nm, indicating conformational changes comparable to those in rabbit skeletal TnC, in agreement with the work of Burtnick, McCubbin and Kay (*Can. J. Biochem.* 53:15, 1975). Stoichiometric titrations in which Ca<sup>2+</sup> was added to EDTA-free cardiac TnC show that two high affinity sites exist, as is the case for skeletal TnC. A plot of fluorescence or CD changes versus free Ca<sup>2+</sup> is steeper than curves corresponding to the binding to a single site, suggesting some interaction between the two sites; the midpoint of the CD and fluorescence transitions occurs at  $4.76 \times 10^{-8}$  M Ca<sup>2+</sup>. The enhancements produced by 2mM Mg<sup>2+</sup> of fluorescence and CD are 55% and 85% respectively of those produced by Ca<sup>2+</sup>. The recently reported amino acid sequence for cardiac TnC (van Eerd and Takahashi, *Biochemistry* 15:1171, 1976) is largely homologous to skeletal TnC and the changes in tyrosine fluorescence suggest that one of the cardiac high affinity sites corresponds to site III (Kretsinger and Barry, *Biochim. Biophys. Acta.* 405:40, 1975). Van Eerd and Takahashi suggest that, because of extensive substitutions, cardiac site I cannot bind Ca<sup>2+</sup>. This leaves only site II or IV as the other high affinity site and suggests that site I of skeletal TnC must be a low affinity site. (Supported by grants from NIH (HL-5949, HL-5811), and the National Science Foundation.

**TH-AM-9 EFFECTS OF AN INTERCHAIN DISULFIDE BOND ON TROPOMYOSIN STRUCTURE.** S.S. Lehrer, Dept. Muscle Research, Boston Biomedical Research Institute, Boston, Mass., 02114.

Our recent studies have shown that reaction of rabbit skeletal muscle tropomyosin (Tm) with Ellman's reagent (Nbs<sub>2</sub>) produces an S-S crosslink between adjacent SH groups of the two  $\alpha$ -helical chains (PNAS 72:3377, 1975). Studies by others have indicated that an S-S crosslink can also be formed by air oxidation. The effects of this specific crosslink on the structure of Tm were investigated by fluorescence and circular dichroism methods as a function of increasing temperature and guanidine hydrochloride concentration, [GuHCl]. Four different preparations of Tm were studied: 1) SH-Tm, Tm reduced with dithiothreitol, 2) IA-Tm, Tm whose SH groups were blocked with iodoacetamide, 3) Nbs-Tm, Tm treated with Nbs<sub>2</sub>, 4) O<sub>2</sub>-Tm, Tm whose SH groups were air oxidized. SDS-polyacrylamide gel electrophoresis indicated that S-S crosslinks were present only in Nbs-Tm and O<sub>2</sub>-Tm. Increasing the temperature or GuHCl concentration at neutral pH produced changes in tyrosine fluorescence, decreases in fluorescence polarization, increases in solute quenching and decreases in ellipticity at 222 nm. All of these measurements showed that non-crosslinked SH-Tm and IA-Tm behaved differently from crosslinked Nbs-Tm and O<sub>2</sub>-Tm. A higher temperature (+8°C) and a greater [GuHCl] (+1M) was required to produce the major structural transition for the cross-linked samples. Reduction of the S-S bond to SH reversed this effect. Also, a minor transition near 1M GuHCl and in the 30-40°C temperature region was observed only for the crosslinked samples. Thus, introduction of a single crosslink between chains at Cys 190 produces a slight destabilization near physiological conditions as well as a large stabilization against total denaturation (supported by grants from NIH (AM1677) and NSF (GB24316)).

**TH-AM-10 LACK OF PHOSPHATE INCORPORATION INTO THE INHIBITORY SUBUNIT OF TROPONIN IN MUSCLES OF LIVE FROG DURING REST AND ACTIVITY.** H. Ribolow\*, K. Bárány, A. Steinschneider\*, and M. Bárány, Departments of Biological Chemistry and Physiology, University of Illinois at the Medical Center, Chicago, Illinois 60612

Despite accumulation of considerable evidence of phosphorylation of the inhibitory subunit of troponin (TN-I) in vitro, no physiological role for this has been demonstrated in skeletal muscle. With the rapid and specific technique of affinity chromatography of TN-I, developed by Syska, et al. (FEBS Letters, 40, 253, 1974), a new approach became available for studying TN-I phosphorylation in muscle. As performed in an 8 M urea containing solution, this method excludes dephosphorylation and proteolysis of proteins during their purification. Affinity chromatography followed by SDS-gel electrophoresis was used in the present work to investigate the phosphorylation of TN-I in muscles of live frogs injected with  $^{32}\text{P}$ -orthophosphate. An incorporation of only 0.0005 mole  $^{32}\text{P}$  per 25,000 dalton of TN-I was found in frogs which were left at 25° after the injection for 3-4 days. Assuming TN-I phosphorylation during muscle contraction, as a result of the increased  $\text{Ca}^{2+}$  concentration in the sarcoplasm, we compared the  $^{32}\text{P}$ -content of TN-I isolated from resting and contracting frog muscles, both frozen in isopentane chilled by liquid nitrogen. No phosphorylation of TN-I could be detected during contraction either. The lack of phosphate incorporation into TN-I both in resting and contracting muscle was also confirmed by another method than affinity chromatography, i.e., by homogenizing and washing the frozen muscles with trichloroacetic acid and by subsequent SDS-gel electrophoresis. These latter methods revealed that several proteins were phosphorylated in live frog muscle. Interestingly, some of these proteins were bound by the troponin C-Sepharose 4B column. (Supported by NS-12172 from NIH, MDA, and MDAC).

**TH-AM-11 STRUCTURE AND PROPERTIES OF BOVINE EMBRYONIC MYOSIN.** Linda Siemankowski\* and A. Stracher, Dept. of Biochemistry, SUNY-Downstate Med. Ctr., Brooklyn, N.Y. 11203.

Previous studies from this laboratory (Dow and Stracher, P.N.A.S. 68, 1106, 1971) have shown that myosin from chick embryonic muscle is deficient in the LC-3 light chain. To examine the consequences of the absence of this light chain, we have studied the properties of myosin from bovine embryonic muscle. Fetuses ranged in age from 120 days to 270 days. Bovine adult myosin appears to have three classes of light chains: LC-1, 25,000; LC-2, 18,000; LC-3, 16,000, regardless of whether it was made in the presence or absence of protease inhibitors. In confirmation of our previous results on chicken embryonic myosin, we have found that bovine fetal myosin has only two classes of light chains: LC-1, 25,000, and LC-2, 18,000. Treatment with DTNB removes 50-80% of LC-2 in the embryonic myosin, with no significant effect on ATPase activity, indicating that fetal myosin is a fast-type myosin even though its specific activity and light chain pattern resemble red or cardiac myosin. The specific ATPase activity at 25 C of bovine adult myosin is 0.4  $\mu\text{mole P}_i/\text{min/mg}$  for Ca, and 2.0  $\mu\text{moles/min/mg}$  for K-EDTA, while the specific activity of bovine fetal myosin is 0.2  $\mu\text{mole/min/mg}$  for Ca and 1.0  $\mu\text{mole/min/mg}$  for K-EDTA. Preliminary data indicate that embryonic myosin heavy chains are more subject to proteolytic breakdown than adult myosin; this degradation of the heavy chains can be followed on SDS gels. Leupeptin, a bacterial protease inhibitor, appears to prevent this degradation. Supported by N.I.H. GM-19626 and M.D.A., Inc.

**TH-AM-12 PROPERTIES OF SCALLOP MYOSIN SUBFRAGMENT-1.** W.F. Stafford, III, E.M. Szentkiralyi, and A. G. Szent-Györgyi, Department of Biology, Brandeis University, Waltham, Mass. 02154.

Myosin subfragment-1 [S-1] has been isolated from the striated adductor muscle of Aequipecten irradians. Washed myofibrils were digested with papain in the presence of calcium and magnesium at pH 7.0, ionic strength 0.12. Gradient elution of crude S-1 from a DEAE Biogel-A column yielded a single component which showed one band in the heavy chain region (92K) on SDS gels and two types of light chains (18K) in stoichiometric amounts on urea gels. About 10% of the mass of the regulatory light chain (RLC) was removed by papain. Actin-activated MgATPase activity of the S-1 had no calcium requirement; however, S-1 retained full calcium binding capacity. Although one of the two RLC's of intact myosin can be removed by EDTA treatment, similar treatment of S-1 does not remove any RLC, indicating that on isolated S-1 the RLC's are attached with uniformly high affinity. The modified RLC could be replaced by purified intact RLC in the presence of EDTA and trace amounts of calcium and magnesium. The modified and intact RLC seem to have similar affinity for isolated S-1. S-1 with restored intact RLC did not exhibit a calcium sensitive MgATPase activity indicating that lack of calcium sensitivity is not due to partial digestion of the regulatory light chain. The relationship of the light chain-S1 interactions to the regulatory process will be discussed.

**TH-AM-13 POLYMERIZATION OF MYOSIN FROM VERTEBRATE SMOOTH MUSCLE.** J. Megerman and S. Lowey, Rosenstiel Basic Medical Sciences Research Center, Brandeis University, Waltham, MA 02154.

The polymerization of smooth muscle myosin was examined by sedimentation velocity and electron microscopy in a study designed to parallel that of Josephs & Harrington (*Biochemistry* 5 (1966) 3474) on skeletal muscle myosin. Myosin from calf aorta (*Fed. Proc.* 35 (1976) 1746) was polymerized by dialysis of the monomer against various [KCl], in 2mM KPi, 1mM EDTA, 0.5mM DTT, pH 6, 7 or 8. The equilibrium that exists between monomer and polymer is qualitatively similar to that reported for skeletal muscle myosin. An increase in polymer concentration is favored by decreasing pH and ionic strength, and the polymer has an intrinsic sedimentation coefficient of about 150 S in 0.2M KCl, pH 7 and 8. However, only a single small polymer species is found even at pH values lower than 7, where skeletal myosin forms several much larger polymers. From measurements of electron micrographs of negatively stained specimens, filament lengths in 0.2M KCl remained nearly constant, at about 0.35 $\mu$ m, regardless of pH. The width of these filaments was variable, with median values ranging from 100 Å at pH 8.1 to 250 Å at pH 6.1. At any given pH, the range of [KCl] in which monomer and polymer remain in equilibrium is higher than for the skeletal myosin system. Under all conditions tested, polymerization occurs at a lower critical concentration of myosin, and the equilibrium concentration of monomer does not remain constant with increasing total protein concentration. We conclude that smooth muscle myosin, which appears more soluble by virtue of its extractability at low ionic strength, is more readily polymerized to small oligomers. These observations, along with a more detailed analysis of electron micrographs (see abstract by Craig & Megerman) suggest that smooth muscle myosin polymerizes in a manner different from that of myosin from striated muscle.

Supported by NIH fellowship HL02278 to J.M. and USPHS Grant AM17350 to S.L.

**TH-AM-14 OBLIQUE FILAMENTS FROM VERTEBRATE SMOOTH MUSCLE MYOSIN.** R. Craig\* and J. Megerman (Intr. by C. Cohen), Rosenstiel Center, Brandeis University, Waltham, MA. 02154.

The assembly of myosin purified from calf aorta muscle (see abstract by Megerman and Lowey) has been studied by electron microscopy of negatively stained specimens. Two distinct modes of aggregation are observed. One is a short bipolar filament (maximum length 0.5  $\mu$ m) similar to that formed from skeletal muscle myosin. Crossbridges are seen at each end of a central bare zone, about 200 nm long, which is formed by the antiparallel overlap of myosin tails running parallel to the filament axis. The second type of aggregate is distinctly different: the tails pack with antiparallel overlaps but run at an angle of 5-20° to the filament axis. An oblique filament is thus formed, having the appearance, in projection, of a parallelogram. Crossbridges lie on the sides that are parallel to the filament axis; they do not appear to be distributed cylindrically around the filament. Bare zones, about 200 nm long, form the other two sides. Filaments elongate by the addition of myosin molecules, or small oblique aggregates, parallel to the bare zones already present. The packing of the tails requires that the crossbridges on opposite sides be directed with opposite sense. This side-polar structure does not appear to have helical symmetry. The short bipolar filaments alone occur at 0.2M KCl, pH 8 but co-exist with side-polar filaments at 0.2M KCl, pH 6 or 7. Side-polar filaments are favoured at 0.3M KCl, pH 6 and grow up to 6  $\mu$ m in length. Similar structures have been observed by Sobieszek (*J.Mol.Biol.* (1972) 70, 741) in preparations from taenia coli, vas deferens and gizzard, suggesting that this is a general mode of aggregation for smooth muscle myosin. Side-polar filaments would have obvious structural advantages over bipolar filaments for producing the large degrees of shortening found in smooth muscle.

Supported by fellowships from Muscular Dystrophy Association (R.C.) and NIH (J.M.)

**TH-AM-15 EVIDENCE OF COOPERATIVE SUBSTRATE BINDING IN SMOOTH MUSCLE MYOSIN.** M.N. Malik and A. Stracher, Department of Biochemistry, SUNY Downstate Medical Center, Brooklyn, N.Y. 11203

Smooth muscle myosin free of actin from chicken gizzards has been purified using column chromatographic procedure to complete homogeneity. The steady state ATPase activity of the purified enzyme was investigated at high and low salt, with and without different divalent cations. An analysis of the substrate saturation curves under these conditions revealed an intermediary plateau region. The double reciprocal plots were non-linear and the Hill plots of these data gave values of  $n=1.5$  and 1 below and above the plateau respectively indicating cooperativity of the substrate binding sites at low substrate concentrations. The plateau was shifted to higher substrate concentrations when the kinetic measurements were made using urea or heat treated enzyme. Also, under these conditions, the cooperativity of the substrate binding site was lost below the plateau but now occurred above the plateau. The cooperativity of the substrate binding sites and the plateau regions were completely lost when the kinetics of the enzyme was carried out at pH 9.0. These results suggest that smooth muscle myosin possesses both positive and negative cooperativity towards its substrate. Supported by grants from American Heart Association and NIH HL 18511 to (M.N.M.), N.Y. Heart Association and HL 14020 to (A.S.). M.N.M. is an Established Investigator of the American Heart Association.

TH-AM-16 SOME FACTORS EFFECTING THE EXTRACTION AND PURIFICATION OF  $\alpha$ -PARAMYOSIN FROM MERCENARIA MERCENARIA. B. D. Gaylinn, W. H. Johnson, L. B. Cooley\*, and L. C. DeMarco\*, Biology Department, Rensselaer Polytechnic Institute, Troy, N.Y. 12181.

It has been shown by Stafford and Yphantis (Biochem. Biophys. Res. Comm. 49: 848, 1972) that paramyosin isolated from Mercenaria mercenaria adductor muscles contains three separate forms designated  $\alpha$ ,  $\beta$  and  $\gamma$ .  $\alpha$ -paramyosin, thought to be the native form, was obtained under conditions which led these authors to suggest that the  $\beta$  and  $\gamma$  forms are degradation products of  $\alpha$ -paramyosin. We have developed several methods of extraction which yield principally  $\alpha$ -paramyosin. A modified acid extraction following the method of Hodge gives good yields. Inclusion of antibiotics in the extraction medium and use of osmotic shock in the initial stages of the ethanol methods of Johnson, et al. (Science, 130: 160, 1959) have given  $\alpha$ -paramyosin in smaller yields. To date all of the methods which we have employed to extract the  $\alpha$  form are consistent with the hypothesis that degradation of  $\alpha$ -paramyosin is the result of the proteolytic activity of marine bacteria carried over from the animal into the extraction steps. We have observed bacterial growth during extraction in procedures which yield  $\beta$  and  $\gamma$  forms. Preliminary evidence strongly suggests that these bacteria are capable of growth in 0.6 M KCl, pH 7.5 and 4°C and that antibiotics which we have employed give protection in short term extractions. We would suggest that the types of marine psychrophilic, halophilic bacteria isolated from shellfish by Colwell and Liston (J. Appl. Micro. 8: 104, 1960) and shown by them to have high proteolytic activity may be responsible for the effects which we have observed and, in addition, may be a complicating factor in extraction of other proteins from tissues of invertebrates from marine habitats.

**TH-AM-B1 SODIUM REPLACES INTERNAL K DURING BATH APPLICATION OF CHOLINERGIC AGONISTS TO ELECTROPHORUS ELECTROPLAQUES.** H.A. Lester, Biology Division, California Institute of Technology, Pasadena, CA 91125.

The innervated face is voltage-clamped in the presence of Ba to block the inward rectifier. In some trials, voltage is varied slowly enough to eliminate Na excitability; such "ramp-clamps" reveal linear current-voltage (I-V) relations. Chloride-free solutions have little transient or permanent effect on the I-V relation; thus the zero-current (resting) potential (-80 to -90 mV) is  $E_K$ . In other trials, Hodgkin-Huxley clamps are applied to measure  $E_{Na}$  (+70 to +150 mV). Agonist is now applied in the bath. This increases the conductance, but only at negative potentials. At positive potentials, the nonsynaptic membrane still completely determines the I-V relation. Ramp clamps show that the nonsynaptic membrane retains its slope conductance but its extrapolated zero-current potential shifts up to 60 mV (dose-dependent) in the positive direction. The shift still occurs in  $Cl^-$  free solutions. Depolarizations by bath-applied agonist are due primarily to this shift of  $E_K$ , not to short-circuiting of  $E_K$  by the agonist-induced conductance. Hodgkin-Huxley clamps reveal a simultaneous, usually larger, negative shift in  $E_{Na}$ . Still in the presence of agonist, hyperpolarizing clamps to -100 mV require large inward currents which, if maintained for 10-20 sec, cause further ( $\sim 20$  mV) shifts of  $E_K$  and  $E_{Na}$ . Upon washing with agonist-free solution, conductances always reverse completely. The shifts of  $E_K$  and  $E_{Na}$  reverse completely after only a few minutes exposure to agonist, incompletely after longer or multiple exposures, and not at all in ouabain or strophanthidin. Thus Na replaces internal K during prolonged exposure to agonists. Batrachotoxin produces similar shifts. Supported by NS-11756 and by MDAA.

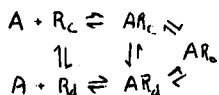
**TH-AM-B2 PURIFICATION AND PROPERTIES OF THE NICOTINIC ACETYLCHOLINE RECEPTOR FROM NORMAL AND DENERVATED SKELETAL MUSCLE.** G. E. Kemp, New York State Dept. of Health, Roswell Park Memorial Inst., Buffalo, N.Y. 14263 and R. J. Bradley, G. B. Brown\*, and G. Robinson\*, Neurosciences Program, The University of Alabama in Birmingham, Birmingham, AL 35294.

We have purified the nicotinic acetylcholine receptor (AChR) from both normal and denervated rat leg muscle. Denervated preparations were obtained from rat hind legs after total denervation for a two week period. The receptor was solubilized in Triton X-100 and initial purification was carried out by  $\alpha$ -cobratoxin affinity chromatography. The receptor was eluted from the affinity column in carbachol and collected on DEAE Sephadex. After a salt elution gradient the receptor was gel filtered on Sepharose 6B. To date, the best preparations of denervated and normal muscle AChR bind 10 and 3 picomoles of  $1^{125}$ - $\alpha$ -bungarotoxin/ $\mu$ g protein respectively. Inhibition of  $1^{125}$ - $\alpha$ -bungarotoxin binding to purified muscle receptor by acetylcholine at concentrations as low as  $2 \times 10^{-8}$  M have been observed. This high affinity acetylcholine binding is known to occur in AChR derived from electric fish electroplax but has not previously been reported for mammalian muscle receptor. A comparison has been made for biochemical and pharmacological properties of the normal and denervated receptor. A variety of agonists and antagonists have been used to study the inhibition of binding of  $1^{125}$  toxin to these preparations.

Supported by USPHS Grant # NS-11356 and NSF BSN 75-14321

**TH-AM-B3 KINETICS OF BINDING OF CHOLINERGIC LIGANDS TO ACETYLCHOLINE RECEPTOR-RICH MEMBRANES.** Jonathan B. Cohen and Norman D. Boyd\*, Dept. Pharmacology, Harvard Medical School, Boston, MA 02115.

Rapid-mixing and ultrafiltration techniques have been used to study directly the kinetics and equilibria characterizing the binding of [ $^3$ H]-acetylcholine (AcCh) to receptor-rich membranes isolated from Torpedo marmorata electric tissue. At equilibrium AcCh is bound with high affinity ( $K_d = 10$ -20nM). However, within 0.1 sec after mixing drug and receptor, AcCh is bound by a receptor conformation characterized by a micromolar dissociation constant, and the conformational transition resulting in high affinity ligand binding occurs only on the second time scale. Analysis of the rate of formation and dissociation of high affinity AcCh-receptor complexes as well as of the effect of competitive and non-competitive antagonists on those processes is used to determine some of the rate and equilibrium constants of the underlying molecular events. The ligand binding properties of the membrane-bound receptor are consistent with the existence of three conformational states:  $R_c$ , the dominant conformation in the absence of ligands;  $R_o$ , the receptor associated with an open channel; and  $R_d$ , the high affinity (desensitized) receptor. The binding of AcCh is interpreted in terms of a cyclic mechanism:



where  $R_c/R_d \geq 20$ ,  $A \cdot R_c/AR_c = 1\mu M$ ;  $AR_c/AR_d = .02$ .

**TH-AM-B4 CHARACTERISTICS OF THE POSTSYNAPTIC CHANNEL AT SNAKE NEUROMUSCULAR JUNCTIONS.**  
 V.E. Dionne, and R.L. Parsons\*, Dept. of Physiology & Biophysics, University of Vermont,  
 Burlington, VT 05401

We have undertaken a preliminary description of the properties of endplate channels at the neuromuscular junctions of grass snakes (sp. *Thamnophis*). Measurements were made on directly visualized twitch fiber endplates of *m. obliquus abdominis externus* maintained in Ringer's (composition (mM): NaCl 159; KCl 2.15; CaCl<sub>2</sub> 1.0; MgCl<sub>2</sub> 4.2; HEPES 1.0; pH 7.2) at 15-17°C. These endplates are compact, about 50  $\mu$ m in extent, so that with a two micro-electrode voltage clamp they are effectively space clamped also. Mean single channel conductance,  $\gamma$ , was estimated by the ratio of the variance of acetylcholine induced endplate current to its mean at known voltages.  $\gamma = 23.4 \pm 4.1$  pS (11); range 18.0 to 31.3 pS (values are mean  $\pm$  S.D. (no. cells)).  $\gamma$  showed no apparent voltage dependence between -110 and +20 mV. The reversal potential,  $V_r$ , of the endplate current was directly observed, not extrapolated.  $V_r = -5.8 \pm 4.4$  mV (14); range -1 to -15 mV. This does not correspond to the equilibrium potential of any major ion present, suggesting that several ions carry the endplate current. These ions appear to share the same endplate channel for the following reason. The variance of the endplate current at  $V_r$  is zero within the accuracy of our measurements. This value is predicted if all ions move through the same channel but not if separate, independent populations of channels exist for each ion. Ionophoretic injection of acetylcholine intercellularly just beneath the postjunctional membrane induced no conductance change; chemical activation occurs from the outside only. These properties are similar to those of the endplate channel at the neuromuscular junction of frog twitch fibers. Supported by USPHS Grant NS 12306-02.

**TH-AM-B5 ACETYLCHOLINE RECEPTOR MEDIATED ION FLUX IN ELECTROPLAX MEMBRANE VESICLES.**

J.P. Andrews\*, G.E. Struve\*, S. Lipkowitz\* and G.P. Hess, Section of Biochemistry, Cornell University, Ithaca N.Y. 14853

Excitable membrane vesicles have been isolated from crude homogenates of electroplax from *Electrophorus electricus* (G.P. Hess and J.P. Andrews, *Proc. Nat. Acad. Sci. USA* 00, 000 (1977)). Sodium and potassium ions within these microsacs are exchanged with ions in the external solution in the presence of acetylcholine receptor ligands. Under appropriate conditions the efflux of ions follows a single exponential decay. The dependence of the first order rate constant,  $k_{obs}$ , for  $^{22}\text{Na}^+$  and  $^{86}\text{Rb}^+$  efflux on either carbamylcholine or decamethonium concentration has been measured and indicates a direct relationship between binding of ligands and receptor-mediated ion flux. d-Tubocurarine was found to be a non-competitive inhibitor of agonist-induced  $^{22}\text{Na}$  efflux indicating separate binding sites for activators and inhibitors of neural activity.

We have investigated the influence of metal ion concentrations on the inside and outside of the vesicles. Under conditions which resemble those in nerve cells, the kinetics of ion efflux becomes biphasic and we observe an initial very fast flux rate. This observation together with the determination of acetylcholine receptor-mediated ion flux through microsome membranes allows a comparison between flux measurements in these vesicles and electrophysiological measurements with nerve and muscle cells. The efficiency of the receptor-mediated process can adequately account for the electrophysiological results.

**TH-AM-B6 REVERSIBLE DEPLETION OF SYNAPTIC VESICLES IN K<sup>+</sup> DEPOLARIZED JUNCTIONS**

Dorothy T. Rutherford\*, William L. Nastuk, and Joseph F. Gennaro Jr.\* Laboratory of Cellular Biology, New York Univ. and Dept. of Physiology, Columbia Univ., New York City

The study of the fate of synaptic vesicle (SV) membrane after the release of neurotransmitter and the source of new vesicles is complicated by the very rapid rate at which the vesicles are replaced. We have found that high extracellular K<sup>+</sup> (potassium propionate) produces rapid depletion of SVs from motor nerve terminals. Cutaneous pectoris nerve-muscle preparations from *Rana pipiens* were completely depleted of SVs after a 30 min exposure to high K<sup>+</sup> soln. (115 mM). Large vacuoles (cisternae) seen in these nerve terminals have previously been described in depleted terminals. These cisternae are believed to be the accumulation of the used SV membrane (Heuser & Reese, 1973, *J. Cell. Biol.*, 57:315). After a 60 min exposure to high K<sup>+</sup>, the nerve terminals contain many coated vesicles in addition to the cisternae. Invaginations of the presynaptic membrane between the active release zones are frequently seen and they appear to be continuous with cisternae. Spontaneous miniature endplate potentials can be recorded 10 min after returning a 30 min depolarized preparation to normal Ringer soln. After 20 min recovery cisternae are still seen and small accumulations of SVs appear. These vesicles are often found associated with the active release zones. After 60 min recovery the nerve terminals closely resemble the control preparations. Adding glucose and choline to the Ringer solution does not enhance recovery. The morphological evidence suggests that the cisternae which are found in depleted nerve terminals are invaginations of the presynaptic membrane, and are not the product of coalescing coated (pinocytotic) vesicles since, in the sequence of depletion, the formation of cisternae precedes the appearance of coated vesicles. NIH-NS04988



**TH-AM-B7 COMPARISON OF THE EFFECTS OF CARBON MONOXIDE AND ANOXIA ON THE ELECTRICAL ACTIVITY IN MAMMALIAN TISSUE CULTURES.** M. Raybourn,\* W. Schimmerling,\* C.A. Tobias, and T.C. Yang,\* Donner Laboratory/Lawrence Berkeley Laboratory, University of California, Berkeley, Ca. 94720

Roller-tube tissue cultures from rat cerebellum are being used to assess carbon monoxide (CO) toxicity relative to that due to anoxia alone. This non-hemoglobin preparation allows a direct comparison of CO and anoxia-mediated cellular dysfunction. Both liquid and gas-phase anoxic insults (100% N<sub>2</sub>) result in varying degrees of disruption of the spontaneous bioelectric activity in most cerebellar Purkinje cells. Gas-phase CO insults (250 to 30,000 ppm) result in a dose-dependent perturbation of this activity. At high doses ( $\geq 1\%$  CO), a complete inhibition of cellular activity usually occurred from which recovery was generally possible. Photodissociation reduces the effects of CO on cellular respiration as manifest in the spontaneous activity. Preliminary data indicate a CO toxicity over and above that due to anoxia, per se, which is surprising in light of the higher affinity of oxygen than CO for cytochrome oxidase.

This research was supported by ERDA/EPA Award DS-E681.

**TH-AM-B8 SPECIFICITY FOR PATTERNED FLASH OF ASYMMETRY IN CORTICAL EVOKED POTENTIAL FOLLOWING STROKE.** R.H. Jacob, V.D. Deshmukh\* and J.S. Meyer\* Department of Neurology, Baylor College of Medicine, Houston, Texas 77030.

We have compared interhemispheric asymmetry (AY) of the averaged cortical evoked potential in response to strobe flash between a group of normal volunteers and patients suffering from cerebral lesions following stroke. When a lesion is present, we find a large AY between hemispheres for the averaged response (potential difference between left or right occipital lead and ear-lobe reference) when stimuli consist of patterned flashes in the lower visual field near the horizontal meridian. For each subject 128 responses to 10-20  $\mu$ s duration flashes were averaged from each hemisphere under three conditions: 1) The stimulus consisted of a row of 1° subtense round holes flashed in a dark background along a horizontal line 5° below the horizontal meridian, the stimulus alternating to either left or right of a central fixation point. (Left-flash and right-flash responses averaged separately.) 2) Same as the first condition except 32° below the horizontal meridian, resulting presumably in a more medial primary cortical response. 3) Diffuse stimulus presented with subject's eyes closed. 300 ms response epochs beginning 50 ms post-stimulus were evaluated on an area basis by locating a central baseline for each response and measuring AY between left and right hemisphere responses as a dimensionless ratio obtained from the area between responses and the total response area. In patients, AY is maximal for condition 1) (patterned flash) and minimal for condition 3) (diffuse flash). AY is generally minimal in normals. The degree of asymmetry appears related to the location of the lesion with reference to the primary cortical response for patterned stimuli.

**TH-AM-B9 CORTICAL POTENTIAL AND SOURCE DISTRIBUTION AROUND A DISCRETE EPILEPTIC FOCUS.** L. Zablow, A.M. Salazar\*, and E.S. Goldensohn\*, Neurology Department, College of Physicians and Surgeons, New York, N.Y. 10032.

A small discrete epileptic focus, made by letting penicillin in a Ringer's solution diffuse from the lumen of a  $\frac{1}{2}$  mm ID capillary tube placed on cat sensorimotor cortex, produces recurrent focal spikes of approximately 100 msec duration. These stabilize in form after about  $\frac{1}{2}$  hour when recorded from the same capillary tube used as an electrode. Additional recordings are made using glass microelectrodes at 36 or more standard locations distributed throughout a rectangular area  $3\frac{1}{2}$  mm in depth and lateral distance from the focus. At each site, averages of sixteen spikes are computed. Similar records are obtained in the cortex directly below the site of placement of the penicillin containing electrode, shortly after its removal. At these locations, monophasic negative spikes are seen at all depths, having a maximum amplitude at 1-1 $\frac{1}{2}$  mm below the surface. Moving laterally, at the surface, the negative spikes decrease in amplitude and are preceded by a positive component of increasing prominence. This biphasic configuration is seen above cortical depths of about 200  $\mu$ m, below which the positive phase disappears and, as it does at the focus, the amplitude of the negative phase goes through a maximum with increasing depth. The Laplacian of the potential field is computed to yield the generator distribution, and displays of potential field and generator current density are presented.

**TH-AM-B10 THE EFFECT OF LOW LEVEL X-RADIATION ON THE LEARNING ABILITY OF PLANARIA.** R. L. Buchanan\*, A. W. Gooch, Jr.\*, W. G. Buckman\*, (Intr. by T. P. Coohill) Western Kentucky University, Bowling Green, Ky. 42101

Planaria (*Dugesia tigrina*) were exposed to low-level radiation before being conditioned using classical learning techniques. Light was used as the conditioned stimulus and electrical shock as the unconditioned stimulus. Five groups containing eight planaria each were exposed to 0.0, 2.5, 5.0, 9.2, and 16.8R (0.0R being the control group). The planaria showed a decrease in trained responses with increased radiation levels above two standard deviations. This study confirmed a preliminary study with three groups of light at 0.0R, 1.0R and 10.0R.

**TH-AM-B11 A MODEL FOR THE MAPPING OF BRAIN ACTIVITY;** P. Anninos, and S. Zenone\*, Physics Dept Concordia University and Physics Dept. Dawson College, Montreal, P.Q.

A more rigorous development of our previously published model for the EEG (Intern. J. of Theor. Phys. VI2,1,1975) will be presented based on the physical and anatomical characteristics of the brain. In such a model the brain tissue is assumed to be an isotropic, diffusive medium in which are uniformly embedded, through, a great many univoltage generators, i.e.: neurons and glia. We also assumed that the passive elements in such medium are only capacitive or resistive. Starting with Maxwell equations for isotropic media and assuming a field derivable from both a scalar and vector potentials we derive a diffusion equation with parameters  $C, \epsilon, \sigma, \mu$ , appearing in the equation being the known capacitance, permittivity, conductivity, permeability respectively for the medium. A solution is then found for the diffusion equation in terms of an expansion up to the second order Bessel's function. This solution represents a Fourier expansion for the EEG at any point, under the hypothesis that the EEG is the summand of all potentials from all the generators embedded in the brain tissue. Our aim is to match the coefficients of such expansion with those of real EEG data. By virtue of the found solution the coefficients are related to the parameter  $\delta$  which is a function of the previously defined physiological parameters. Consequently the sources of variation among the coefficients between individuals and various types of mental activities are capable of being directly related to the changes in  $\delta$ . Comparison of the corresponding coefficients for the same individuals under similar kind of mental activity will be made. With that we expect to acquire a new coordinate system characteristic for the particular individual under particular mental activity.

**TH-AM-B12 SIMULTANEOUS RECORDING FROM 14 NEURONS IN THE SUPRAESOPHAGEAL GANGLION OF THE BARNACLE USING A NEW POTENTIAL SENSITIVE DYE.** A. Grinvald\*, B.M. Salzberg, L.B. Cohen, K. Kamino\*, A.S. Waggoner, C.H. Wang\* and D. Ti\*, Dept. of Physiology, Yale University, New Haven, CT. 06510 and Dept. of Chemistry, Amherst College, Amherst, MA.

Using giant axons from the squid, *Loligo pealii*, we have tried 113 additional dyes in a search for larger changes in absorption or fluorescence that are potential dependent. One of these dyes, 5-[(1- $\gamma$ -triethylammonium sulfopropyl-4-(1H)-quinolylidene)-2-butenylidene]-3-ethyl-2-thio-2,4-oxazolidinedione, (NK2367), a merocyanine-oxazolone, had a signal-to-noise ratio in an absorption measurement that was twice as large as the previous best signal. This dye was used to monitor electrical activity of individual neurons in the ganglion of the giant barnacle, *Balanus nubilus*, using an ordinary microscope and collecting the light from the magnified real images of neurons at the objective image plane with light-guides that were glued to photodiodes. Action potentials from individual neurons were optically recorded with a signal-to-noise ratio of greater than 10:1 and, under the best circumstances, synaptic potentials with an amplitude of only 4 mV were also monitored optically. This dye did not cause any photodynamic damage in barnacle experiments and obvious pharmacological effects were not observed. Using 14 separate electrooptical recording units we were able to monitor electrical activity from 14 neurons simultaneously. In one experiment 7 of the monitored neurons made 81 spontaneous action potentials during 2 seconds of recording. We hope that this apparatus can be expanded so that most of the neurons in the ganglion can be monitored simultaneously. (Supported in part by USPHS grants NS 08437, NS 10489 and MH 27853, and an EMBO long term fellowship to A.G.)

**TH-AM-B13 CHANGES IN INTRACELLULAR  $\text{Ca}^{2+}$  DURING PACEMAKER ACTIVITY IN A MOLLUSCAN NEURON MEASURED WITH ARSENAZO III.** M.V. Thomas\* and A.L.F. Gorman, Department of Physiology, Boston University School of Medicine, Boston, Mass. 02118.

Changes in free intracellular  $\text{Ca}^{2+}$  were measured in the neuron R-15 in the abdominal ganglion of *Aplysia* during spontaneous bursting pacemaker activity. The soma was injected with the  $\text{Ca}^{2+}$ -sensitive dye Arsenazo III and changes in dye absorbance were used to detect changes in  $[\text{Ca}]_i$ . We find that  $[\text{Ca}]_i$ , but not  $[\text{Mg}]_i$ , increases during each burst of action potentials and that this increase occurs primarily in steps coincident with each action potential. The absorbance changes associated with each burst were greatly reduced by lowering  $[\text{Ca}]_o$  from 10 mM to 1 mM and by salines with normal  $[\text{Ca}]_o$  (10 mM) containing 10 mM  $\text{Co}^{2+}$  or  $\text{Mn}^{2+}$ . These results suggest that most of the increase in  $[\text{Ca}]_i$  during the burst occurs as a result of  $\text{Ca}^{2+}$  influx rather than from release from intracellular stores. We calculate that the total increase in  $[\text{Ca}]_i$  during the burst is approximately  $5 \times 10^{-8}$  M. Intracellular  $\text{Ca}^{2+}$  injections which produce absorbance changes of comparable size hyperpolarize the cell. In voltage clamped cells, the time course of the outward current produced by intracellular  $\text{Ca}^{2+}$  injection corresponds to the time course of the absorbance change. Our results suggest that the increase in  $[\text{Ca}]_i$  is sufficient to cause the hyperpolarization which follows each burst and that the interval between bursts is determined by the rate of decline of  $[\text{Ca}]_i$ . This research supported by NIH Grant NS11429.

**TH-AM-B14 EFFECTS OF FCCP AND VALINOMYCIN ON CATECHOLAMINE UPTAKE INTO CHROMAFFIN GRANULES: EVIDENCE FOR COUPLING OF CATECHOLAMINE TRANSPORT TO A pH GRADIENT.** R.W. Holz, Behavioral Biology Branch, National Institute of Child Health and Human Development, National Institutes of Health, Bethesda, Md. 20014

It is known that ATP and  $\text{Mg}^{2+}$  stimulate catecholamine uptake into chromaffin granules, the catecholaminergic storage vesicles from adrenal medullary cells. Recent studies indicate that chromaffin granules have an internal pH over 1 unit more acid than the medium (Johnson, R.G. and A. Scarpa. 1976. *J. Biol. Chem.* 251: 2189-2191). Furthermore, there is evidence that the ATPase associated with the chromaffin granules is responsible for the pH gradient (Bashford, C.L., G.K. Radda and G.A. Ritchie. 1975. *FEBS Lett.* 50: 21-24). To investigate the possibility that catecholamine transport may be coupled to the pH gradient, the effect of collapsing the pH gradient on catecholamine transport was examined. The  $\text{H}^+$  transporter, FCCP, and the specific  $\text{K}^+$  carrier, valinomycin (val), were used. It was found that FCCP alone (0.05-0.1  $\mu\text{M}$ ) had little or no effect on catecholamine uptake. This would be expected if collapse of the pH gradient requires countertransport of a + permeant cation. Val (10-20  $\mu\text{M}$ ) alone also had no effect in the presence of either  $\text{Na}^+$  or  $\text{K}^+$ . The combination of FCCP and val had no significant effect in the presence of 0-57 mM  $\text{Na}^+$ . However, FCCP and val in the presence of  $\text{K}^+$  (20 mM) inhibited uptake by approximately 50%. Thus when the  $\text{H}^+$  gradient was presumably collapsed by  $\text{H}^+$ - $\text{K}^+$  exchange, catecholamine uptake was inhibited. The inhibition of uptake could not have been caused by lysis of chromaffin granules since less than 3% of the total releasable catecholamine was released. These ionophore effects are preliminary evidence in support of the notion that catecholamine transport is coupled to the pH gradient.

**TH-AM-B15 VESTIBULAR PHYSIOLOGY OF SPASTIC AXOLOTL.** C.F. Ide\* (Intr. by M. Larrabee), Department of Biophysics, Johns Hopkins U., Balto., MD 21218.

The spastic mutant axolotl (*Ambystoma mexicanum*) shows deficient swimming and equilibrium. Behavior "phenocopy" experiments implicated the vestibular projection to the cerebellum in mutant behavior patterns. Here I report single unit recordings, carried out in the vestibulo-cerebellum (auricle) of wild type and mutant animals in response to natural vestibular stimulation. Six vestibular unit types responding to rotation or tilt about the longitudinal axis were encountered in both animal types. However, where 85% of wild type units found in the superficial auricle (0-300  $\mu\text{m}$ , including the Purkinje cell zone) responded to rotation or tilt, only 60% were found to do so in the spastic. The mutant auricle contained 25% more units spontaneously active in the horizontal (level) position. Spastics also showed a dramatic change in location of units responding to sustained ipsilateral tilt. Where all of these units occurred below 300 microns in depth in the cerebellum of mutants, only 52% were found in this deep zone in wild type, the remaining units occurring in the superficial cerebellar zone. Electrical stimulation experiments showed this superficial zone to be the major area of projection of the anterior ear nerve in wild type animals. These data, in conjunction with anatomical findings, suggest an altered morphogenesis of hindbrain cerebellar structures in spastics. (NIH Grant MH-13445)

TH-AM-B16 COMPETITIVE RETINOTECTAL MAPPING IN XENOPUS. R.K. Hunt, Jenkins Biophysical Labs., Johns Hopkins Univ., Baltimore, MD 21218.

Retinal ganglion cells use unique locus-specific properties to discriminate 'targets' in the optic tectum and assemble a retinotectal map. Studies of abnormal connectivity after partial ablations (as when half-retina spreads its map over whole tectum), aiming for the 'mapping rules' by which these properties operate, have been plagued by the possibility of surgery-induced changes in the properties themselves: a 'redifferentiation' of surviving cells to embrace a full range of properties, much as embryonic fields 'regulate' to make whole small organs. Here I report that when eye growth is permanently halted by early larval treatment with Fluorodeoxyuridine, the resultant tiny eye (whose 1-4000 ganglion cells would have been clustered around the optic disc of the normal adult retina and occupy but a small patch of the map) usually (17 of 19 cases) maps over most of the tectum. When a normal eye (with complete set of fibers & specificities) is made to superinnervate the same tectum (concurrent with, before or after the tiny eye), the tiny eye's fibers are 'chased' from most of the tectum to a small patch at the lateral edge, which they share with peri-disc fibers of the normal eye. I conclude that (retinal) specificities and (tectal) targets cross-react, and site selection is a competitive operation. (Supported by NIH Grant NS-12606 & NSF Grant BMS-75-18998)

**TH-AM-C1 SOLUBILITY OF n-ALKANES IN PLANAR BILAYER MEMBRANES.** Stephen H. White, Department of Physiology, University of California, Irvine, CA 92717.

Measurements of the specific geometric capacitance ( $C_g$ ) of planar bilayer membranes as a function of temperature have been made under equilibrium conditions. Bilayers were formed from glycerol-1-monolein and a series of n-alkanes (hexane through octadecane). Alkane was always present in excess resulting in saturation equilibrium between microlenses and true bilayer. Therefore, the bilayer was treated as a saturated solution of alkane "solute" in bilayer "solvent." The amount of alkane in the bilayer determines in part the thickness of the bilayer and consequently  $C_g$ . The mole fraction ( $X_g$ ) of alkane as a function of temperature (T) can be calculated from the  $C_g(T)$  data. From the resulting  $X_g(T)$  data, the enthalpies ( $\Delta H$ ) and entropies ( $\Delta S$ ) of transfer of alkanes from bulk (i.e., microlenses) to bilayer can be estimated (S. H. White, *Nature*, 262 (1976), 421). These estimates permit a direct thermodynamic comparison between bilayer interior and bulk alkane. Some of the  $\Delta H$  found are  $-130 \pm 79$  cal/mol (octane),  $-55 \pm 44$  cal/mol (decane),  $+1.02 \pm 0.1$  Kcal/mol (tetradecane),  $+3.82 \pm 0.36$  Kcal/mol (octadecane).

This research was supported by grants from the N.S.F. (GB-40054) and the N.I.H. (NS-10837). S.H.W. is a Research Career Development Awardee of the N.I.H. (NS-00146).

**TH-AM-C2 INTERACTION OF BUTYLATED HYDROXYTOLUENE (BHT) WITH PHOSPHOLIPID BILAYER MEMBRANES.** M.A. Singer, Department of Medicine, Queen's University, Kingston, Ontario, Canada. K7L 3N6

BHT is extensively used as a food preservative presumably because of its antioxidant properties. This molecule accumulates in the body, most likely in fat compartments since it is very lipid soluble. (Hexane to water partition coefficient exceeds 2000 to one). Although BHT is considered non-toxic, several studies have revealed significant effects on biological membranes. Since a proposed site of action of BHT is the hydrocarbon core of the membrane, a study was undertaken to examine the interaction of this agent with phospholipid bilayers. Liposomes were formed from dipalmitoyl phosphatidylcholine (PC), dimyristoyl PC, or a mixture of the two. Such vesicles display a marked increase in Na22 efflux in the temperature region of the  $T_c$  of their constituent phospholipid. Whereas the local anesthetic dibucaine shifts the onset of this permeability maximum to a lower temperature, BHT in contrast, eliminates the increase in Na22 efflux. The hydroxyl group of BHT appears important with respect to this effect since an analogue missing this group does not prevent the increase in Na22 efflux. Although dibucaine and BHT have dissimilar effects on Na22 permeability, both "fluidize" the bilayer and lower the  $T_c$  of the phospholipid as measured in spin labelled liposomes. Since this fluidizing effect of BHT should increase Na22 efflux, the observed decrease in sodium permeability indicates that this molecule perturbs the bilayer in some additional manner (perhaps involving an alteration in surface dipole potential). (supported by the MRC)

**TH-AM-C3 SOLUBILITY OF CHAINED MOLECULES IN LECITHINS.** S. Simon Duke University Department of Physiology and Y. Katz University of Miami Department of Pharmacology, Miami Florida, 33152.

A method for estimating freedom of movement in phospholipid lamella is suggested. The method is based on comparing free energies, entropies and enthalpies of solution of hydrocarbons like hexane in hydrophobic solvents like benzene and hexadecane with the corresponding thermodynamic functions in phospholipid membranes.

The theoretical basis for the method is an extension of a theory used to explain solubility of noble gases in phospholipid to hydrocarbon solutes. Entropies and enthalpies of solution of hexane in lecithins near the phase transition were found to be about three fold than in typical hydrophobic solvents like benzene. At higher temperatures the difference vanishes. This was shown to be due to restrictions on the rotational freedom of movement of the solute caused by the restrictions on the phospholipid structure. These restrictions are eased at a higher temperature. Further comparison with bulk hydrocarbon solvents revealed limitations to the use at these solvents as models to membranes. The theory was further used to predict solubilities in the hydrophobic and hydrophilic regions of the phospholipid membranes.

**TH-AM-C4 MECHANICAL THEORY FOR FUSION OF VESICLES WITH CELL MEMBRANE SURFACES.** E.A. Evans, and M.J. Costello, Depts. of Biomed. Eng. and Anatomy, Duke University, Durham, NC 27706.

A thermo-mechanical theory for fusion of single bilayer vesicles with the bilayer component of cell surfaces has been developed. The theory is based on changes in free energy from: (1) the contact of the outer lipid layers; (2) the initial creation of a point defect in the outer lipid layers plus the subsequent circular enlargement; and (3) the curvature produced by the evagination of the inner lipid layers. Contact of the outer lipid layers results in a reduction,  $\Delta F_s$ , in the interfacial free energy density of interaction between water and an outer layer. The free energy density required to create and enlarge a circular defect in the contact region is equal to the surface pressure,  $\Pi_0$ , in an outer layer. Because it is assumed that the hydrocarbon interior of the bilayer is incompressible, expansion of a circular defect in the outer layer produces a commensurate local evagination of the inner layer. The induced curvature produces a bending moment or curvature elastic effect due to the change in interaction between amphiphiles (e.g. repulsive forces); if the amphiphile-amphiphile interaction is assumed to be distributed uniformly along part of the amphiphile length,  $h_p$  (e.g. the polar head group height), then the bending or curvature elastic coefficient would be:  $K_1 \cdot h_p^2 / 12$  (where  $K_1$  is the area compressibility modulus,  $-A(\partial \Pi_1 / \partial A)_T$ , for an inner layer). Minimizing the total free energy yields equations of equilibrium for the system which, limited by the amphiphile packing constraints, will yield the geometry of the fusion region. These equations show that complete fusion should occur when:  $|\Delta F_s + \Pi_0| \sim h_p^2 \cdot K_1 / h^2$  (where  $h$  is the total bilayer thickness). Since the outer layer surface pressure is essentially equal to the free energy density of water-hydrocarbon interaction, the reduction in interfacial free energy density must exceed the free energy density of the hydrophobic effect by the curvature elastic energy density.

**TH-AM-C5 PHOSPHOLIPID VESICLES AS CARRIERS FOR ANTI TUMOR DRUGS: PHARMACOKINETICS IN VIVO.** R. L. Juliano, Research Institute, The Hospital for Sick Children, Toronto, Ontario.

We have studied the formation, stability and biological fate of liposome encapsulated anti tumor drugs including Actinomycin D (AD), cytosine arabinoside (ara C), daunomycin (DA) and vinblastine sulfate (VBS). Non polar drugs such as AD, VBS, and DA are efficiently entrapped in liposomes and probably form a complex with the liposomal membrane. Polar drugs such as ara C are entrapped within the aqueous compartments of the liposomes. The liposome-drug complexes are extremely stable in the case of non polar drugs and little loss of drug (0.1 - 0.5% / hr) is observed in vitro. In the case of ara C the liposome-drug complex is less stable and approximately 3-5% of the drug is lost per hour. Encapsulation within liposomes radically alters the pharmacokinetics of anti tumor drugs in vivo. Thus for example the half time for clearance of free daunomycin on the rat is less than 5 min, while the half time for clearance of liposome encapsulated daunomycin is several hours. The tissue disposition of anti tumor drugs is also substantially modified by liposome encapsulation with generally greater drug retention in all tissues but especially in those tissues rich in reticuloendothelial elements such as lung, spleen and liver.

**TH-AM-C6 Laplace Plane Analysis of Dynamic Electrochemical Phenomena at Living Cell Surfaces.** Arthur A. Pilla\*, Intr. by Shu Chien, Bioelectrochemistry Laboratory, Orthopaedic Research Laboratories, Columbia University, College of Physicians & Surgeons, N.Y., N.Y. 10032.

Electrochemical information transfer in vivo is based on the concept that specific potential dependent interactions at a cell's interfaces involving such charged species as divalent cations, and hormones are key steps in determining cellular function. This approach has guided studies in bone physiology wherein selective modification of  $Ca^{2+}$  binding and protein synthesis has been achieved by a highly specific dynamic injection of charge at the cell's interfaces. These findings have already been translated into the clinic with a high success rate in incurable fracture healing. This study describes a working model for electrochemical information transfer using a detailed analysis of the transient electrical behavior of living cell membranes. The approach focuses on the interactions of the charged components of a cell's interfaces with their respective charged environments as dynamic electrochemical events. It is shown that by considering the total transmembrane current as composed of both charging,  $i_c$ , and phase transfer,  $i_p$ , currents a unified approach to membrane impedance may be established. Both  $i_c$  and  $i_p$  are coupled so that the dynamic charging requirements related to mechanistic models for phenomena as diverse as gating in excitable membrane transport or a modification in membrane-hormone activity in non-excitable systems may be established. Utilizing this approach Laplace transformation techniques have allowed the isolated toad urinary bladder to be studied over the frequency range 1Hz to 10MHz. Results show that the rate controlling step for  $Na^+$  transport is interfacial phase transfer and that the time constant for this event is unusually long (>1msec) indicating that a substantial potential dependent specific modification in interfacial structure must occur as opposed to simple charge rearrangements governed by purely electrostatic phenomena.

TH-AM-C7 EVIDENCE FOR DIELECTRIC SATURATION OF THE AQUEOUS PHASES ADJACENT TO CHARGED BILAYER MEMBRANES. C.-C. Wang\* and L.J. Bruner, Dept. of Physics, University of California, Riverside, CA. 92502.

The relationship between solution concentration of dipicrylamine anion,  $C_{aq}(DPA^-)$ , and the surface density,  $Q_s$ , of  $DPA^-$  adsorbed to dioleylecithin membranes has been determined, with  $Q_s$  being measured by a high field voltage jump method.<sup>1,2</sup> The Gouy-Chapman theory for symmetric indifferent electrolyte ( $z^+ = -z^- = z$ ) states that for low surface potential ( $ez|\psi_s|/kT \leq 1$ ) we have  $Q_s \propto C_{aq}(DPA^-)$ , while for surface potentials of greater magnitude  $Q_s \propto [C_{aq}(DPA^-)]^{z/(z+2)}$ , the sublinearity resulting from electrostatic repulsion of impinging  $DPA^-$  ions by those already adsorbed. On log-log plots these asymptotes yield straight lines which intersect at  $Q_s = \sqrt{2\epsilon\epsilon_0 kT c_0}$  (in MKS units) where  $c_0$  is the concentration of indifferent electrolyte. The predicted sublinear power law dependences of  $Q_s$  upon  $C_{aq}(DPA^-)$  have been observed for  $NaCl$  [ $z/(z+2) = 1/3$ ] and for  $MgSO_4$  [ $z/(z+2) = 1/2$ ] over a range of salt concentrations from  $10^{-4}M$  to  $1.0M$ . At  $c_0 = 10^{-4}M$  the experimentally determined value of  $Q_s$  may be used to calculate  $\epsilon \sim 80$  from the above theory. As the salt concentration is increased, however, this calculation yields progressively lower values of dielectric constant, with  $\epsilon \sim 3$  at  $c_0 = 1.0M$ .

This work was supported by the United States Army Research Office.

1. Bruner, L. J. 1975. *J. Membrane Biol.* 22 : 125.
2. Andersen, O.S., and M. Fuchs. 1975. *Biophys. J.* 15 : 795.

TH-AM-C8 THE EFFECT OF SURFACE CHARGE ON INTERFACIAL ION TRANSPORT. M. Blank and J.S. Britten\*, Department of Physiology, Columbia University, 630 W. 168 St., New York, N.Y. 10032.

Recent experiments have shown that the rate of ion flow through monolayers and bilayers varies with the surface charge density of the layer and the ionic strength of the aqueous solutions. In the monolayer study (Miller and Blank - *J. Coll. Interface Sci.* 26:34, 1968), surface charge was varied by the adsorption of a charged surfactant at a mercury/water interface, and the rate of passage of an ion through this surface film was measured polarographically. In the bilayer experiment (Sweeney and Blank - *J. Coll. Interface Sci.* 42: 410, 1973), the surface charge was varied by changing the concentration of a soluble surface active ion in the adjacent aqueous phases, and the DC resistance to  $NaCl$  solutions was then measured. The observed dependence of ion transport on the surface charge in the two systems can be explained by assuming that electrical double layer theory describes the distribution of ions near an interface during ion flow. According to this view, the resistance due to the ultra-thin layer arises because of the exclusion of ions of the same charge from the electrical double layer region. The effect is therefore a partition phenomenon, rather than a variation of the diffusion coefficient through the layer. The agreement between the two sets of observations and the derived equations suggests that electrical double layer theory is useful for describing systems that are not far from equilibrium. In addition, the ability to account for ion transport through monolayers and bilayers in this way suggests that the explanation also applies to related processes in natural membranes. (Supported in part by NSF PCM 76-11676.)

TH-AM-C9 SURFACE CHARGE DETECTION OF PHOSPHOLIPID VESICLE INTERACTIONS WITH PLANAR BILAYER LIPID MEMBRANES. J.A. Cohen and M.M. Moronne\*, Laboratory of Physiology and Biophysics, Univ. of the Pacific, San Francisco, Calif. 94115.

The antibiotics Nonactin, Valinomycin, and Monazomycin have been used to detect the interaction of anionic phospholipid vesicles (liposomes) with planar bilayer lipid membranes (BLMs). The interactions are sensed by monitoring, in the presence of charged aqueous vesicles, the antibiotic-mediated BLM conductance which is a function of BLM surface-charge density and the BLM current-voltage characteristic whose asymmetry indicates an asymmetry of the acquired surface-charge distribution. It is found that liposomes containing anionic phosphatidylserine (PS), when added to the aqueous phase, impart negative surface charge to zwitterionic phosphatidylcholine (PC) and phosphatidylethanolamine (PE) BLMs. If added to one aqueous compartment only, PS liposomes deposit negative surface charge asymmetrically, mainly on the vesicular side of the BLM. This surface charge is irreversibly incorporated into the BLM, since it cannot be removed by perfusion of the vesicular aqueous compartment. PS liposome-BLM fusion, as generally conceived, should deposit some surface charge on the side opposite to which the liposomes are added. Monazomycin measurements indicate that such effects do not occur for the case of PS liposomes with PC or PE BLMs. For the case of PS liposomes with PC-PS or PE-PS BLMs, treatments known to produce PS liposome fusion (e.g. addition of mM  $CaCl_2$ , then removal with EDTA) do not affect the acquired BLM surface-charge distributions significantly. It is apparent that fusion is not the dominant interaction here; other interactions will be discussed. It is concluded that the requirements for fusion of liposomes with planar BLMs are far more stringent than the requirements now established for fusion of liposomes with one another.

Supported by NIH (HL-16607) and NSF (PCM 76-11950).

**TH-AM-C10 ION CURRENTS IN ASYMMETRIC PHOSPHOLIPID BILAYERS.** B.D. Hansen\*, J.I. Korenbrot†, A. Harris\* (Intr. by R.J. Goerke). Physiol. Dept., U. of Ca., San Francisco, CA 94143

The transbilayer phospholipid asymmetry found in many biological membranes may result in a membrane surface potential asymmetry. Even with symmetric ionic solutions, this potential asymmetry should induce a difference in the ionic concentrations at one membrane-solution interface with respect to the other. If ionic conductance is proportional to the interface ionic concentration, the lipid asymmetry should produce asymmetric current flow (rectification). We show that this is the case by forming asymmetric planar bilayers and measuring currents under symmetric ionic solutions in the presence of neutral carriers (valinomycin & nonactin), an ionic channel (gramicidin) and lipophilic ions (tetraphenylborate & dinitrophenol). **CHARGE-CHARGE ASYMMETRY.** Asymmetric bilayers were formed from two phosphatidylethanolamine, PE, monolayers with one aqueous phase buffered at pH2 (net positive charge, more positive interface) and the other at pH9 (net negative charge, less positive interface). Current rectification consistent with this voltage asymmetry was detected with the neutral carriers. **CHARGE-DIPOLE ASYMMETRY.** Asymmetric bilayers were formed from PE (no net charge, more positive interface) and phosphatidylserine, PS, (net negative charge, less positive interface) monolayers with both aqueous phases buffered at pH7. Current rectification consistent with this voltage asymmetry was detected with all probe systems. The relaxation time constants of tetraphenylborate were also asymmetric. **DIPOLE-DIPOLE ASYMMETRY.** Asymmetric bilayers were formed from phosphatidylcholine, PC, (no net charge, more positive interface) and PE (no net charge, less positive interface) monolayers with both aqueous phases buffered at pH7. The ionic currents recorded using the channel system and the lipophilic ions were rectified as expected. The currents of the two carrier complexes were rectified in a direction opposite than expected. Supported by NIH Grant EY01586.

**TH-AM-C11 BILAYER ASYMMETRY OF LIPIDS AND POLYPEPTIDES.** R.C. Waldbillig and T.J. McIntosh. Dept. of Physiology and Biophysics, University of Texas Medical Branch, Galveston, Texas 77550, and Dept. of Anatomy, Duke University, Durham, North Carolina 27706.

Asymmetrical bilayers have been formed by joining together monolayers of different chemical composition. The ultrastructure of these bilayers has been determined by a combination of electron microscopic and x-ray diffraction methods in which one half of the bilayer was used as a structural reference for the entire bilayer.

EM images of the unstained bilayers and corresponding x-ray derived bilayer absolute electron density profiles (7Å) suggest that head group influences are more important than hydrocarbon factors in the maintenance of asymmetry in bilayers derived from monolayers. Bilayers of opposed Ba and Ca behenate (C<sub>22</sub>H<sub>44</sub>O<sub>2</sub>) remain segregated whereas bilayers of behenate and behenic acid undergo spontaneous self-mixing. Asymmetric bilayers of long chain behenate (C<sub>22</sub>) and short chain palmitate (C<sub>16</sub>) remain segregated with the interior -CH<sub>3</sub> groups located off center. Symmetrical bilayers formed from mixed monolayers of the long and short molecules have one head group plane and a delocalized internal -CH<sub>3</sub> group. This suggests a spontaneous pairing of long and short molecules across mixed bilayers.

Poly-L-lysine stabilizes asymmetrical fatty acid bilayers. The hydrophilic peptide resides in the bilayer polar region but alters the tilt of the hydrocarbon chain.

**TH-AM-C12 LATERAL DIFFUSION COEFFICIENT CHANGES AT THE PHASE TRANSITION IN LIPID BILAYERS.** P. F. Fahey, University of Scranton, Scranton, Pa. 18510, and W. W. Webb, Cornell University, Ithaca, N.Y. 14853

We have measured the lateral diffusion coefficients  $D$  of a fluorescent lipid analog, 3,3'-diocadecylindocarbocyanine iodide (diI) in single and multiple lipid bilayers of dipalmitoyl phosphatidylcholine (DPPC), dimyristoyl phosphatidylcholine (DMPC), and glycerol monooleate (GMO) both above and below the expected hydrocarbon chain ordering phase transition temperatures  $T_c$ . In single bilayers (BLMs) generated by the Montal-Mueller technique [PNAS 69, 4561 (1972)] we found that  $D$  changed by much less than one order of magnitude in DPPC and in GMO between  $T \ll T_c$  and  $T \gg T_c$ . However in oriented, hydrated, multilamellar bilayer liquid crystals of DPPC and DMPC,  $D$  changed by about two orders of magnitude between temperatures well below  $T_c$  and well above it. Above  $T_c$  in multilamellar bilayer liquid crystals  $D \approx 10^{-8}$  cm<sup>2</sup>/sec but above  $T_c$  in BLMs  $D \approx 10^{-7}$  cm<sup>2</sup>/sec in several lipid systems including GMO, DMPC, DPPC and egg lecithin (EPC). Fluorescent indicators suggest that at least local order changes do occur at  $T_c$  in these BLMs. In BLMs of EPC and DPPC generated by the Mueller-Rudin technique [Mueller et al., Nature 194, 979 (1962)] retained, small alkane solvent increased  $D$  by about a factor of two above  $T_c$ . Cholesterol additions can decrease  $D$  by about a factor of two. We used Fluorescence Correlation Spectroscopy to measure diffusion coefficients in BLMs [Magde et al., Biopolymers 13, 29 (1974)] and Fluorescence Photobleaching Recovery to measure diffusion coefficients in the multilamellar bilayers [Axelrod et al., Biophys. J. 16, 1055 (1976)].



**TH-AM-C13** DIFFUSION AND PATCHING OF MACROMOLECULES IN PLANAR LIPID BILAYER MEMBRANES.

D. E. Wolf†, J. Schlessinger‡, E. L. Elson‡, W. W. Webb, R. Blumenthal, P. Henkart‡, Cornell University, Ithaca, N.Y. 14853; N.C.I., N.I.H., Bethesda, Md. 20014 (R.B. and P.H.)

We have developed a model system for biological membranes in which amphipathic macromolecular antigens are bound to planar lipid bilayers. The effect of antibodies on the diffusion and distribution of these membrane-bound antigens has been studied. The antigens used are derivatives of dextran (M.W. 82,000) to which controlled amounts of fatty acid, rhodamine, and the antigenic hapten TNP have been covalently bound. These fluorescent amphipathic antigens bind to artificial planar lipid bilayer membranes from the aqueous medium. The diffusion coefficients of these macromolecules were measured by fluorescence photobleaching recovery. Two levels of membrane-bound antigen were studied: At  $\sim 10^2$  molecules/ $\mu^2$  they were distributed homogeneously and showed a lateral diffusion coefficient  $D = (2.1 \pm 0.9) \times 10^{-8}$  cm<sup>2</sup>/sec. On the addition of anti-TNP small visible clumps formed similar to the "patches" observed on cell membranes. At a higher level of membrane-bound antigen,  $\sim 10^4$  molecules/ $\mu^2$ , the distribution was again homogeneous but lateral diffusion slower with  $D = (3.1 \pm 1.0) \times 10^{-9}$  cm<sup>2</sup>/sec. At this concentration the addition of anti-TNP slowed the diffusion rate but did not cause patching. However, further cross-linking by anti-Ig resulted in a complete cessation of lateral diffusion and at higher concentrations, the formation of patches. Similar phenomena were observed using concanavalin A as the cross-linking ligand. The diffusion of a fluorescent lipid probe was unaffected by either the addition of macromolecules or their subsequent cross-linking. Cross-linking one population of dextran derivatives partially retarded the diffusion of another non-cross-reacting population. Sodium azide, colchicine, and cytochalasin B did not affect the motion of these molecules.

Research supported by NSF #DMR75-04509 (to W.W.W.) and NIH #GM-21661 (to E.E. and W.W.).

**TH-AM-DI WHY DO SOME PROTEINS CRYSTALLIZE FROM 2-METHYL-2,4-PENTANEDIOL?** Serge N. Timasheff and Eugene P. Pittz, Graduate Department of Biochemistry, Brandeis University, Waltham, Mass. 02154.

The crystallization of ribonuclease A from 55% 2-methyl-2,4-pentanediol (MPD) is a puzzle, since MPD is expected to be a good denaturant. In order to elucidate this question, the thermodynamic interactions between ribonuclease A and solvent components were investigated in water-MPD mixtures of various compositions at pH 5.8. The results show that, at all solvent compositions, addition of protein increases the chemical potential of MPD, with a resultant preferential exclusion of MPD from contact with protein. From the interaction parameters obtained, it can be shown that addition of MPD to an aqueous solution of ribonuclease A to a final solvent composition of 55% MPD should result in phase separation, if total protein concentration is higher than 9 mg/ml. The preferential exclusion of MPD from contact with protein is attributed to unfavorable interactions with charged groups on the surface of the protein. (Supported by NIH grants GM 14603, CA 16707, and NSF grant BMS 72-02572).

**TH-AM-D2 CRYSTALLOGRAPHIC STUDIES OF PROTEIN FOLDING.** W. Traub\*, A. Yonath\*, A. Podjarny\*, A. Sielecki\*, B. Honig\*, and J. Moult\* (Introd. by D.A. Torchia) Structural Chemistry, Weizmann Institute, Rehovot, Israel.

Denaturants have been extensively used to study protein unfolding and refolding in solution, but have provided relatively little information about the conformational changes involved. The use of cross-linked triclinic lysozyme crystals has enabled us to investigate some of these changes in detail by means of X-ray structure analysis. Soaking of cross-linked crystals in denaturant solutions of increasing concentrations caused corresponding increases in crystal volume and decreases in minimum observable X-ray spacings. These changes proved partly reversible on diluting the solutions. The effects of various denaturants were studied by following crystal volume and minimum X-ray spacing as a function of concentration, as well as by means of detailed structure analyses at several intermediate stages in the denaturation and renaturation cycles. It appears that at least two different denaturation mechanisms are involved, with detergent-like reagents disrupting the hydrophobic interactions joining the two wings of the lysozyme molecule and hydrophilic denaturants interacting primarily with polar groups on the molecular surface. These studies have also indicated that denaturant-mediated conformational changes involve relative movements of fixed domains in the protein structure.

**TH-AM-D3 FIBRINOPEPTIDE B AND AGGREGATION OF FIBRINOGEN.** John R. Shainoff, Research Div., Cleveland Clinic, Cleveland, OH 44106

It is now possible to remove fibrinopeptide B without fibrinopeptide A from rabbit, bovine, and human fibrinogen. Copperhead venom procoagulant enzyme, previously shown to remove B faster than A, has been found to release little A at temperatures below 14°. At low temperatures, tight aggregation of the derivative lacking B blocked release of A by the enzyme. Transient release of A occurred, but stopped as removal of B approached completion. Overall losses of A amounted to 8% and 2% from human and rabbit fibrinogen, respectively. Resultant clots with A intact dissolved on warming to 37°, whereafter release of A resumed with secondary coagulation ensuing. When dissolved at 37° with PMSF-inactivated enzyme, the fibrin remained highly soluble (>12 mg/ml). Ultracentrifugation showed constant levels of 8S monomer together with 16S aggregates in amounts accounting for the total protein at concentrations down to 0.16 mg/ml, and monomer alone at lower concentrations. From changes in saturation level of monomer at lower temperatures, the enthalpy of aggregation appeared to be of the order of -20 kcal/mole, approximately half that known to be associated with aggregation of fibrin lacking both fibrinopeptides. Other experiments indicate that removal of the two peptides unmasks separate aggregation sites, each of which place the monomers in an alignment necessary for crosslinking by factor XIIIa. The formation of 16S aggregates through release of peptide B contrasts with the well known formation of 24S aggregates on removing either A alone or both A and B. To explain this difference, it is suggested that removing A promotes aggregation of monomers in a double stranded array while B masks sites for strengthening binding within the strands. With peptide A intact, aggregation may be limited to alignment of monomers in a single stranded array.

**TH-AM-D4 FLUORESCENCE STUDIES OF PROTEIN BOUND TO POLYMER SURFACES.** B.D. Fair\*, Department of Macromolecular Science, Case Western Reserve University, Cleveland, Ohio 44106 and W.B. Rippon, Department of Chemistry, Walla Walla College, College Place, Wash. 99324

The cascade process leading through to the intrinsic clotting of blood is in many instances initiated by Hageman Factor (HF, Factor XII), a plasma protein. Activation of this protein induces the rest of the blood clotting scheme and has been reported to result from contacts with a negatively charged surface. Absorption of HF onto ellagic acid, a known activator, leads to a conformational change in this plasma protein such that previously unexposed hydrophobic regions become exposed to the environment. This conformational change has been characterized by fluorescence spectroscopy and the use of an extrinsic hydrophobic fluorescent probe, 1,6-diphenyl-1,3,5-hexatriene (DPH). Also, upon activation a marked decrease in HF intrinsic fluorescence was observed. These findings have paved the way in determining what type of conformational changes, if any, occur with the contact or absorption of HF on suspensions of polyamino acids being considered for implant purposes. Such techniques may have application as a screening process for suitable implant materials.

Work was supported by Research Grants HLB 15195 and HLB 01661.

**TH-AM-D5 A SYNTHETIC POLYELECTROLYTE MODEL FOR HYDROPHOBIC FOLDING OF BIOPOLYMERS: POLY(METHACRYLIC ACID) CHAIN.** S. Ponratnam\*<sup>1</sup> and S.P. Rao\* (Intr. by A.K. Wright) Dept. of Biochemistry, University of Tennessee Center for the Health Sciences, Memphis, TN 38163. <sup>1</sup>National Chemical Laboratory, Poona, INDIA.

Special features of aqueous solution copolymerization of ionizing monomers were investigated in terms of their free radical reactivity ratios as function of pH, with a view to synthesize methacrylic acid (MAA) copolymers as simpler models for the study of hydrophobic folding in biopolymers. The pH induced conformational transition of copolymers of MAA and a nonionic hydrophilic monomer, N-vinylpyrrolidone (NVP) of different compositions (2-35% NVP) was followed by potentiometric titration and viscosity. The hydrophobic collapse observable for pure poly(methacrylic acid) (PMAA) at low degrees of ionization ( $0 < \alpha < 0.3$ ) disappeared at NVP contents  $> 16$  mole%, as shown by the conformational free energy data. The results indicate that long range methyl-methyl hydrophobic contacts are insufficient to bring about a collapse of the PMAA chain and a minimum average sequence length of about 20 MAA units is required to compact the molecule. Hydrophilic shielding of the methyl groups by the intervening NVP segments could also destabilize the folded structures.

**TH-AM-D6 THE UNFOLDING AND REFOLDING BEHAVIOR OF RIBONUCLEASE S AND OF 7-FTC-LYS RIBONUCLEASE S.** A.M. Labhardt, J.A. Ridge, R.L. Baldwin, Department of Biochemistry, Stanford University, Stanford, CA 94305

The unfolding and refolding kinetics of ribonuclease S (RNase S) have been studied in the pH range 2-7, together with the equilibrium transition curves for thermal unfolding. A chromophoric derivative, 7-FTC-Lys-RNase S has also been studied: it contains a fluorescein thiocarbamyl label attached to lysine 7 of the S-peptide. At pH 7, the transition curve for thermal unfolding of 7-FTC-Lys-RNase S is biphasic when monitored by the FTC label, but closely resembles that of RNase S when monitored by the absorbance of the buried tyrosine groups. In stopped-flow, pH-jump, studies of the refolding of RNase S, three refolding reactions are seen both by tyrosine group absorbance and by binding of the specific ligand 2'CMP. The absence of any concentration dependence of the kinetics suggests that recombination of S-peptide with S-protein is fast compared to these three first-order reactions, whose time constants are 80 msec, 2 sec, and 70 sec, respectively at pH 6, 23°. The 2'CMP binding results indicate that native RNase S is formed in each of the three reactions. The simplest explanation appears to be that there are three unfolded forms of S-protein, analogous to the two unfolded forms of ribonuclease A.

**TH-AM-D7 DETERMINATION OF THE ENTHALPY OF DENATURATION BY MICROCALORIMETRY AND THE DENATURATION OF PHYCOCYANIN IN UREA SOLUTION.** C-H. Chen\*, O. H. W. Kao\*, and D. S. Berns, Division of Laboratories and Research, New York State Department of Health, Empire State Plaza, Albany, NY 12201

The enthalpy of denaturation of phycocyanin was investigated by employing microcalorimetry to measure the heats of mixing of phycocyanin and urea solutions. The protein is completely denatured in a 7 M urea solution. In the denaturation range, there is a sharp increase in the negative enthalpy. The overall enthalpy of denaturation is calculated to be -230 kcal/mole. This relatively large negative enthalpy of denaturation contains contributions from the dissociation of protein into its  $\alpha$  and  $\beta$  subunits, protein unfolding, and changes of protein solvation. The complete denaturation of phycocyanin in 7 M urea was confirmed by ultraviolet and visible spectroscopy, circular dichroism and sedimentation equilibrium. The ultraviolet and visible spectra of phycocyanin demonstrate that the maximum absorption at 625 nm shifts to a lower wavelength in the presence of urea. The optical density at the maximum absorption decreases as the urea concentration ( $C_u$ ) increases and levels off at  $C_u \geq 7$  M. Measurements show that the strong positive band of the protein at  $\sim 630$  nm shifts to 600 nm at  $C_u = 2-10$  M. The molar ellipticity at 222 nm remains unchanged at  $C_u = 0-4$  M, decreases at  $C_u = 5-7$  M and remains essentially of the same magnitude at  $C_u = 7-10$  M. Sedimentation equilibrium measurements demonstrate that in 7 M and 8 M urea solutions, the mean molecular weight of phycocyanin subunits is 14,000 daltons, which is not far from one-half of the monomer molecular weight of 30,000 daltons of phycocyanin.

**TH-AM-D8 THERMAL INSTABILITY AS A DETERMINANT OF PHYSIOLOGICAL ENZYME TURNOVER.** Roger Bonomo\* and Horton A. Johnson, Department of Pathology, Tulane University School of Medicine, New Orleans, La. 70112

There is no satisfactory explanation for the rapid renewal rates of intracellular enzymes, some of which have half-lives of a few hours or less. We have investigated the possibility that thermal denaturation of these proteins at physiological temperatures may be a major factor in their rapid turnover. We measured the rates of thermal denaturation of the two enzymes of rat liver: soluble malate dehydrogenase and membrane bound cytochrome c reductase. Denaturations were carried out in intact tissues and in tissue homogenates. Rates of thermal inactivation were measured at temperatures of 40-54°C. In each case inactivation rates followed the Arrhenius law, allowing extrapolation to 37°C. Our data show that:

- 1.) The strong temperature dependence of inactivation rates indicates denaturation as a mechanism.
- 2.) Membrane bound cytochrome c reductase shows significantly more thermal stability within the cell (in liver slices) than in homogenate.
- 3.) Thermal stability is extremely variable from one enzyme to another. The projected half-life at 37°C of soluble malate dehydrogenase is 23 days; that of cytochrome c reductase is only 4.5 hours.
- 4.) The estimated turnover of cytochrome c reductase due to thermal denaturation is comparable to that measured by isotope decay, suggesting that the rapid turnover of intracellular enzymes may simply reflect the maintenance of a steady state in the presence of thermal noise.

**TH-AM-D9 CIRCULAR DICHROISM STUDIES AND REACTIVITY OF BOVINE PARATHYROID HORMONE.** S.F. Andres\*, R. Zand, and D.S. McCann\*, Biophysics Research Division, Institute of Science and Technology, Department of Biological Chemistry, University of Michigan, Ann Arbor, Mich. 48109, and Wayne County General Hospital, Eloise, Mich. 48132

Circular dichroism spectroscopy was used to determine the secondary structure of the native 84 amino acid residue bovine parathyroid hormone and of the synthetic parathyroid hormone fragment (residues 1-34) in aqueous and trifluoroethanol solvent. The spectra of the peptide and protein in water are interpreted as showing that the major component of secondary structure is the random coil (60-80%) with a moderate amount of  $\beta$  structure (20-40%) and only 0-10%  $\alpha$  helix. In trifluoroethanol solvent the  $\alpha$  helical content is increased to about 25% for both substances. Boiling aqueous solutions of the peptide or the protein yields a decrease in both biological and immunological reactivity as assayed by a cyclic AMP generating system and by radioimmuno assays directed towards the carboxyl and amino terminal portions of these molecules respectively. Thus, the presence of the  $\beta$  conformation appears to be essential for the biological activity of both the peptide and the protein since material that has been treated at 100°C suffers about a 50% loss in activity when assayed in both tests.

Supported by N.I.H. grants AM 18680, NS 11923 and the Wayne County General Hospital MSR and E fund.

**TH-AM-D10 THE FLEXIBILITY OF HUMAN IMMUNOGLOBULIN A1 ( $\kappa$ ) MYELOMA PROTEIN.** B. M. Liu, H. C. Cheung, J. Mestecky\*, and S. C. Harvey, Biophysics Group, Department of Microbiology, University of Alabama in Birmingham, Birmingham, Alabama 35294

The flexibility of human monomeric IgA1 ( $\kappa$ ) myeloma protein labelled with dansyl chloride (DNS) was studied by using the nanosecond single photon detection technique. The time course of the emission anisotropy of the IgA1-DNS complex was recorded after excitation with a linearly polarized light pulse. To calculate the net emission anisotropy the number of stray photons caused by protein scattering was subtracted from the total number of photons detected in the IgA1-DNS complex. The rotation correlation times and the corresponding coefficients were estimated by a nonlinear parameter estimating program by use of the method of least squares. Results indicated that the anisotropy decay curve could be expressed by the sum of two exponential functions:  $A(t) = C1 \cdot \exp(-t/T1) + C2 \cdot \exp(-t/T2)$ , with  $C1 = 0.042 \pm 0.004$ ,  $C2 = 0.249 \pm 0.004$ ,  $T1 = 9 \pm 2$  ns, and  $T2 = 198 \pm 15$  ns (means and standard errors,  $N=7$  experiments). The existence of a sizeable component with a short decay time leads us to conclude that contrary to Weltman and Davis (J. Mol. Biol. 54: 117, 1970), the human IgA1 myeloma protein is flexible. The site of flexibility in the IgA1 system is currently studied in our laboratory.

(Supported in part by NIH grants AM-14589, GM-42596, and AI-19854).

**TH-AM-D11 PSEUDO-DYNAMIC SURFACE ACCESSIBILITY CALCULATIONS: CORRELATION OF AMINO ACID SIDE CHAIN ACCESSIBILITIES AND SOLVENT TRANSFER FREE ENERGIES:** Michael H. Klapper, J.D. Gellis,\* Department of Chemistry, The Ohio State University, Columbus, Ohio 43210

A new algorithm has been used to compute solvent accessible surface areas of N-acetyl amino acid esters. Conformations are generated by assigning to appropriate bonds random dihedral angles, and discarding structures with internal overlaps. Solvent accessibilities of the remaining conformers are determined atom by atom. A test sphere, representing water, is placed randomly on the noncovalent surface of an atom. The accessible surface area is computed to any desired accuracy from the fraction of placements having no overlaps between the test sphere and the molecule. The total accessible area is the sum of the atom contributions. The distribution of accessible areas over all generated conformers is non-Gaussian, and relatively wide (e.g., for alanine: mean  $15.07 \text{ \AA}^2$ , variance  $1.45 \text{ \AA}^2$ , range  $7.67 \text{ \AA}^2$ ). The mean areas of aliphatic side chains are linearly correlated with the amino acid ester transfer free energies from organic liquids to water (P.K. Nandi, Int. J. Peptide Protein Res. 8, 253, 1976) with a slope of ca.  $100 \text{ cal}/\text{Å}^2$ . The computed means are affected only slightly by weighting the conformations with a Boltzmann factor based on accessible surface area. The use of this area-transfer free energy correlation to estimate the magnitude of apolar bonding in proteins will be discussed.

**TH-AM-D12 ON THE CORRELATION OF FREE ENERGIES OF TRANSFER OF PEPTIDES FROM A NON-POLAR TO AQUEOUS MEDIUM WITH SURFACE AREAS.** V. Renugopalakrishnan, \*Dept. of Chemistry, Rutgers, The State University of N.J., Newark, N.J. 07102.

Surface areas of a number of peptides: N-acetyl L-amino acid N-methyl amides of glycine, alanine, serine, threonine, leucine, valine, histidine, phenyl alanine and tyrosine were calculated using the method suggested by Hermann (J. Phys. Chem., 76, 2754, 1972). In the above procedure for the calculation of surface areas each atom i is regarded as a sphere of radius  $r_i$ , where  $r_i$  is given by the Van der Waals radius. Peptides were assumed to exist in the energetically preferred backbone and side chain conformations determined from conformational energy calculations (V. Renugopalakrishnan, S. Nir and R. Rein, to be submitted). A linear relationship has been obtained between the surface areas and the experimental values for the free energies of transfer determined by Nozaki and Tanford (J. Biol. Chem., 246, 2211, 1971). The problem of hydrophobicity will be discussed from the preliminary results obtained in the study.

\* Present Address : Lab. of Molecular Biophysics, Univ. of Alabama Medical Ctr., Birmingham, Alabama 35294.

**TH-AM-D13 KINETICS OF FATTY ACID BINDING TO HUMAN SERUM ALBUMIN.** W. Scheider, Biophysics Research Division, Institute of Science and Technology, University of Michigan, Ann Arbor, Michigan, 48109

Early results of a kinetic study of the binding of fatty acid to human serum albumin suggest that one step in the process occurs with a rate constant of the order of  $2 \text{ sec}^{-1}$  in mixtures which are about 0.5 mM each in defatted protein and oleic acid. The method of the study involves repeated application of short square pulses of electric field to monitor the polarizability of the protein molecules in solution during the binding, which is initiated in a conventional stop-flow apparatus fitted with an electrode chamber.

**TH-AM-D14 STRUCTURE:VOLUME RELATIONSHIPS. FUNCTIONAL DEPENDENCE BETWEEN THE SPECIFICITY OF PROTEIN:ION INTERACTION AND ASSOCIATED VOLUME EFFECTS.** Sam Katz and R. Shinaberry,\* Biochemistry Dept., West Virginia Univ. School of Medicine; Morgantown, West Va. 26505

Binding of a metal effector to an apoenzyme involves its coordination to several ligands in a unique domain; the associated conformational change transforms the inactive protein to a functional operator. One approach to study this is to determine the volume changes produced when the 'correct' and 'incorrect' cations are added to the apoenzyme. A novel approach is to use difference dilatometric titrations, i.e., determining the  $\Delta V$  produced by the incremental addition of cations to form  $M_n \cdot P$  complexes ( $n = 1, 2, 3, 4 \dots$  moles of cation, M, per mole of protein, P). To resolve these volume effects in terms of cation:ligand coordination processes, electrostatic contributions and conformational changes a vocabulary must be established. Consequently, we determined the  $\Delta V$  for the coordination of Cu(II) and Zn(II) to such ligands as carboxylates, amines, imidazoles, peptides, etc. This study deals with the  $\Delta V$  produced by the reaction of these cations with globular proteins of differing compositions and binding affinities.

Cu(II) associating with lysozyme, ovalbumin and bovine serum albumin produced strikingly different volume effects as a function of the binding sites. The formation of 1:1 Cu(II):protein complexes of lysozyme, ovalbumin and bovine serum albumin produced volume changes of 11, 28 and 35 ml/mole, respectively. The  $\Delta V$  for the lysozyme complex is explainable by Cu(II) complexing to a carboxylate residue; a conclusion verified by X-ray crystallographic analysis. For serum albumin the volume effects agree with chemical data indicating a multidentate coordination with a carboxylate, a peptide backbone and imidazole residues. Parallel studies performed in 8 M urea delineate the contribution of the proteins conformation to the binding process.

**TH-AM-D15 RUTHENIUM RED: USE OF RESONANCE RAMAN SPECTRA TO PROBE  $\text{Ca}^{++}$  BINDING SITES IN BIOLOGICAL SYSTEMS.** D. L. Rousseau,\* J. M. Friedman, Bell Laboratories, Murray Hill, New Jersey 07974, and G. Navon, Institute of Chemistry, Tel-Aviv University, Ramat-Aviv, Israel.

Ruthenium red (RR) has become increasingly useful in biological studies since it has been found to inhibit certain  $\text{Ca}^{++}$  dependent processes. Most extensively studied has been the effect on  $\text{Ca}^{++}$  uptake and transport in mitochondria upon addition of RR but other systems have shown  $\text{Ca}^{++}$  uptake inhibition as well. In spite of the amount of work done with RR in biological systems, an understanding of the binding mechanisms are lacking. For that reason we have initiated a Raman investigation of RR. In this preliminary study we found the following: 1) The Raman spectrum of RR exhibits a strong resonance enhancement with visible wavelength excitations. This enhancement allows for detection of RR at very low concentrations ( $< 10^{-4} \text{ M}$ ). 2) Different Raman spectra are observed depending on whether RR is unbound, bound to chelating agents (EDTA, EGTA), or bound to specific proteins. These differences can be observed in room temperature spectra as well as  $6^\circ \text{K}$  spectra. The binding appears to be stoichiometric. 3) A concentration of  $\text{Ca}^{++}$  of approximately 10 times that of RR is required to re-obtain the unbound RR spectrum in the presence of equimolar EDTA. 4) Based on the Raman spectrum, RR does not appear to bind to lipids. From this study we conclude that resonance Raman scattering studies of RR bound to biological substances may help to elucidate the nature both of the  $\text{Ca}^{++}$  binding in proteins and of the inhibitory effect of RR on processes requiring  $\text{Ca}^{++}$ .

**TH-AM-D16 THE EFFECT OF pH AND IONIC STRENGTH ON THE ACTIVITY OF RIBONUCLEASE A.** M.R. Eftink\* and R.L. Biltonen,\* Department of Biochemistry and Pharmacology, University of Virginia School of Medicine, Charlottesville, Virginia, 22901. Introduced by D.B. Kupke.

The activity of Ribonuclease A is known to be ionic strength dependent. An analysis of the pH dependence of the enzymatic activity as a function of ionic strength (using cyclic-CMP as substrate) has demonstrated that the influence of ionic strength is largely a result of shifts in the pK<sub>a</sub>'s of the functional histidine residues both in the free and complexed enzyme. The pH independent rate constant  $k_2$  is found to remain virtually constant from ionic strength 0.05 to 1.0 M. The  $K_m$  for cyclic-CMP is found to have a much greater dependence on ionic strength. Studies also show that at all ionic strengths, the  $K_m$  becomes very large (approaches  $0.5 \text{ M}^{-1}$ ) at high pH values where the active site histidines are deprotonated. This fact suggests that the affinity of the substrate at lower pH is primarily due to electrostatic interaction with the protein. Consistent with this conclusion is that the fact that  $\Delta H$  for substrate binding is significantly less favorable than for the binding of either cytidine or 3'CMP. These results support the conclusion that electrostatic interactions are of major importance during the catalytic reaction.

**TH-AM-D17 THE A PROTEIN OF BACTERIOPHAGE fd: ITS ISOLATION AND CHARACTERIZATION.** T-C Lin\*, and I. J. Bendet, Department of Life Sciences, University of Pittsburgh, Pittsburgh, PA 15260.

<sup>3</sup>H-His labeled fd was disrupted in SDS-dithioerythritol-Tris buffer, and its A protein separated by SDS Sephadex column chromatography. After being concentrated and rerun through the column, the A protein was exhaustively dialyzed against Tris-HCl buffer at pH 7. Analysis of the amino-acid composition of the A protein showed that it is rich in Gly, Ala, Ser, Thr, Asp(n), poor in Try, Cys, and Met, and based upon a molecular weight of 72,200 daltons, has only 3 His. This molecular weight would agree with our results from SDS gel electrophoresis, in which purified A protein traveled at only a very slightly lower rate than the calibration standard BSA(MW 68,000). Determination of the extinction coefficient,  $E_{0.1\%}^{276\text{nm}}$ , has yielded somewhat variable results: 0.81 obtained from the dry weight, 1.24 as derived from the weight indicated by the amino-acid analysis, and 1.0 to 1.1 based upon observed interference fringe displacements during sedimentation. The yield of A protein from the column was 0.00407 absorbance units at 276nm per absorbance unit at 260nm of fd added. Assuming extinction coefficients for the A protein and virus of  $E_{0.1\%}^{276\text{nm}} = 1.05$  and  $E_{0.1\%}^{260\text{nm}} = 3.74$ , respectively, one fd virion of 14,600,000 molecular weight (Berkowitz and Day, J.Mol.Biol. 102, 531, 1976) would contain 210,000 daltons of A protein, or the equivalent of three monomers. Sedimentation equilibrium of the A protein, in 0.1 M Tris-HCl, 0.014 M  $\beta$ -mercaptoethanol, pH 9, indicated a major oligomer species of 218,000 daltons, assuming a partial specific volume of 0.715, as calculated from its amino-acid composition. Recently, the A protein in 0.1 M Tris-HCl, pH 7, has been shown to interfere with fd infection of the host bacterium. (Lin and Bendet, BBRC 72, 369, 1976).

**TH-AM-D18 THE INTERACTION OF ACRIDINE DYES WITH VIRUSES AND THEIR COMPONENTS.** P. Bricker, I. J. Bendet, Department of Life Sciences, University of Pittsburgh, Pittsburgh, PA 15260.

Fluorescence measurements were made on acridine dyes in the presence of viruses and their isolated nucleic acids in order to determine the accessibility of the latter to interaction with acridines. Double stranded DNA (synthetic poly-dAdT, calf thymus DNA, T4-DNA), single stranded NA (fd-DNA, TMV-RNA), TMV, fd bacteriophage and TMV protein were added to either acridine orange (AO) or quinacrine hydrochloride (QHCl), and the fluorescence recorded as a function of the nucleic acid to dye ratio (P/D). The experiments, carried out in either 50 mM or 0.5 mM phosphate buffer at pH 6.5, were done at 2°C to maximize the fluorescence. For nucleic acid added to AO there is an initial decrease in the fluorescence at low values of P/D. At higher P/D values AO exhibits an enhanced fluorescent intensity regardless of the nucleic acid added. The fluorescence of QHCl, however, is enhanced only by poly-dAdT and is quenched by the other nucleic acids. High ionic strength shifts the curves toward higher P/D values, suggesting that both weak and strong modes of binding are affected. In that whole virus decreases the fluorescence of the dyes to about the same degree as the viral protein, independent of the effect the free nucleic acid would have, it would appear that the acridines cannot interact directly with the nucleic acids of TMV or fd through their protein coats.

**TH-AM-E1 ENHANCEMENT OF POST REPLICATION REPAIR FOLLOWING UV IRRADIATION OF MAMMALIAN CELLS BY PRETREATMENT WITH IONIZING RADIATION.** R. B. Setlow and Eleanor Grist, Biology Department Brookhaven National Laboratory, Upton, New York 11973.

The newly synthesized DNA in UV-irradiated mammalian cells is smaller than that synthesized in unirradiated cells. During a subsequent incubation the small pieces are elongated and eventually give rise to parental size molecules in a process called post replication repair (prr). In bacteria, prr is associated with error-prone repair and a part of it is inducible by treatments that inhibit DNA synthesis. In mammalian cells prr may be enhanced by small doses of UV or the chemical carcinogen N-acetoxy-2-acetylaminofluorene<sup>1,2</sup>. The enhancement was largest for cells of xeroderma pigmentosum (XP) variants--cells proficient in excision repair but defective in prr. Our experimental procedure involved exposing aerobic cells, whose DNA was labeled by overnight incubation with <sup>14</sup>C-dThd, to x-rays (0 or 1000R). The cells were incubated for 3h, exposed to a UV dose (254nm) or 0 or 5Jm<sup>-2</sup>, and shortly thereafter pulsed with <sup>3</sup>H-dThd (0.2 - 1h) followed by a chase of 0 or 1h. The DNA was analyzed by sedimentation in alkali and the fraction of <sup>3</sup>H under the peak of parental <sup>14</sup>C-DNA was taken as a measure of post replication repair. X-irradiation alone has little effect on the size of pulse labeled DNA with or without a chase, but x-rays markedly enhance the amount of prr after a subsequent UV dose to cells of XP variants or to Chinese hamster (V79) cells. We observed little enhancement in an XP of complementation group A. These data lend support to the idea that treatments that inhibit DNA synthesis enhance prr in XP variants. Work supported by the U. S. Energy Research and Development Administration.

- 1) R. B. Setlow and E. Grist, Biophys. J. 16, 183a (1976).
- 2) S. M. D'Ambrosio and R. B. Setlow, PNAS 73, 2396 (1976).

**TH-AM-E2 REPAIR OF PYRIMIDINE DIMERS IN ULTRAVIOLET-IRRADIATED *CHLAMYDOMONAS*.** G.D. Small and C.S. Greimann\*, Biochemistry Section, Division of Biochemistry, Physiology and Pharmacology, The University of South Dakota School of Medicine, Vermillion, So. Dak. 57069

The single-celled green alga, *Chlamydomonas reinhardtii*, has been suggested as a useful model eukaryotic cell for studying DNA repair. Several mutants sensitive to UV-light have been isolated which have been suggested to be deficient in the dark-repair of UV-induced pyrimidine dimers. However, Swinton and Hanawalt failed to find any evidence of excision of pyrimidine dimers when irradiated wild-type cells were incubated for 24 hr under non-photoreactivating conditions. We have re-examined this question using a UV-specific endonuclease to monitor the presence of pyrimidine dimers in the DNA. All of the dimers induced by 50 J/m<sup>2</sup> of 254 nm light are removed by a 2 hr exposure to photoreactivating light. Nearly all of the dimers are removed by the wild-type strain of *Chlamydomonas* upon incubation for 24 hr in the dark. Two UV-sensitive mutants, UVS1 and UVS6, are deficient in removal of dimers in the dark. These results are interpreted to mean that *Chlamydomonas* has an excision-repair pathway for coping with UV-induced damage. [Supported by NIH grant GM 21095.]

**TH-AM-E3 DEFECTIVE EXCISION AND POST REPLICATION REPAIR IN A *recL* MUTANT OF *E. coli* K-12.** R. H. Rothman\*<sup>1,2</sup> and A. J. Clark\*<sup>3</sup> (Intr. by P. M. Achey), <sup>1</sup>Department of Genetics and <sup>2</sup>Department of Molecular Biology, University of California, Berkeley, 94720. <sup>3</sup>Present address: Department of Biology, Brookhaven National Laboratory, Upton, N. Y. 11973.

The *recL152* mutation of *E. coli* was isolated as a recombination deficient, UV sensitive derivative of a *recB<sup>-</sup>recC<sup>-</sup>sbcB<sup>-</sup>* strain. A *recL152* single mutant, however, is Rec<sup>+</sup> but remains UV sensitive. We have explored the possibility that *recL* plays a negligible role in recombination but operates in a major pathway of repair after UV irradiation.

The *recL* mutation leads to a reduction of excision repair as measured by an increase in the time required to close *uvrA-uvrB* mediated incision breaks, and by a reduction of host cell reactivation ability. Postreplication repair is also delayed when measured in a *uvrB5 recL152* double mutant. Such a determination could not be made using the *recL152* single mutant because the excision defect led to an accumulation of nicks in the unlabelled high molecular weight DNA to which the labelled DNA synthesized after irradiation must attach in order to achieve normal high molecular weight. Further, we present evidence to show that the *recL* gene product is required to rejoin gaps in undamaged parental strand DNA which are generated during postreplication repair, and that such gaps accumulate in a *recL152 uvrB5* double mutant. We have noticed a striking phenotypic similarity between *recL152* and *polA1* and suggest that *recL152* is required for the *in vivo* activity of DNA polymerase I.

R.H.R. was supported by U. S. Public Health Service Training Grant No. GM367-16. This research was supported by U. S. Public Health Service Research Grant No. AI05371 from the National Institute of Allergy and Infectious Diseases.



**TH-AM-E4 VARIATION OF UV SENSITIVITY OF A BACTERIAL SYSTEM WITH CHANGING DNA CONTENT.**

D. G. Walbridge\* and B. V. Bronk, Physics and Microbiology Departments, Clemson University, Clemson, SC 29631

*E. Coli* B/r (ATCC 12407) were grown to log phase in a series of media known to provide a range of doubling times, and hence DNA content which increases with decreasing doubling time.<sup>1,2</sup> Log phase cells ( $5-8 \times 10^7$  cells/ml) grown in the various media were irradiated in a nutrient free salt solution at ice temperature and plated on nutrient agar for comparison. The slope of the exponential portion of the semi-logarithmic survival curve remains roughly constant at about  $100 \text{ [ergs/(mm)}^2\text{)]}^{-1}$ . The zero dose intercept however increases markedly as the DNA content increases.

1. Helmstetter, C. E. and Cooper, S., *J. Mol. Biol.* **31**, 507. (1968).
2. Hucul, J. A. Masters Thesis, Niagara University. (1976).

**TH-AM-E5 RECOMBINATION OF UV-INDUCED PYRIMIDINE DIMERS IN HUMAN FIBROBLASTS.** R. Waters<sup>1</sup>, and J. D. Regan\*, Biology Division, Oak Ridge National Laboratory, Oak Ridge, TN 37830.

By using an UV endonuclease assay the recombination of UV induced pyrimidine dimers (pyr [ ]pyr) into DNA synthesized after irradiation has been monitored in fibroblasts from normal patients and those suffering with xeroderma pigmentosum, Fanconi's anemia or ataxia telangiectasia. (<sup>14</sup>C) dThd labeled cells were UV irradiated, and sampled immediately for the number of UV endonuclease sites induced, or pulse labeled with (<sup>3</sup>H) dThd and chased in unlabeled medium. DNA was then extracted and assayed for UV endonuclease sensitive sites. The induction and excision of pyr [ ]pyr resembled that already seen for these cell lines. The number of UV endonuclease-sensitive sites found in DNA synthesized after the irradiation of the excision-deficient XP cells increased linearly with UV dose from  $5-30 \text{ J.m}^{-2}$ , at least 5% of the sites induced in the parental DNA being exchanged. Half this number were found to be exchanged in normal cells which, however, have excised 50% of the pyr [ ]pyr by this time. If one assumes that recombined dimers are equally accessible to excision in normal cells, the exchange of these lesions has occurred at the same frequency in both normal and XP excision deficient fibroblasts. Cells from patients suffering with Fanconi's anemia or ataxia telangiectasia exhibited exchange frequencies ranging from 7-10% and are not significantly different from those obtained with normal cells. These results indicate that a percentage of pyr [ ]pyr can be found in the DNA of human cells that is synthesized after irradiation. The mechanism responsible for this exchange operates in both normal, Fanconi and ataxia cells. The XP result indicates that the process is independent of the incision step required for the excision of pyr [ ]pyr in normal cells. (Research supported by NCI and U.S.ERDA under contract with the Union Carbide Corporation.) <sup>1</sup>P.D.I. supported by subcontract No. 3322 from the Biology Division, ORNL, to the Univ. of Tenn.

**TH-AM-E6  $\gamma$ -RAY MUTAGENESIS IN RADIATION SENSITIVE STRAINS OF YEAST.** R. H. McKee\* and C. W. Lawrence, Department of Radiation Biology and Biophysics, University of Rochester, Rochester, NY 14610

Studies of the action of UV irradiation on the yeast *Saccharomyces cerevisiae* have identified three repair pathways. An investigation of the reversion frequency of a defined mutation in the structural gene for cytochrome C suggest that UV mutagenesis results from the processing of UV damage by a single "error-prone" repair pathway. Mutations at least seven loci (*rad6*, *rad8*, *rad9*, *rad18*, *rev1*, *rev2*, and *rev3*) block at least some type of mutational event, although only the *RAD6* and possibly *REV3* gene products appear to be necessary for all UV mutational events at all sites in the genome.

In the present study the  $\gamma$ -ray induced reversion frequency of the ochre mutation *cyc1-9* was measured in twenty diploid yeast strains homozygous for different, nonallelic radiation sensitive mutations.  $\gamma$ -ray reversion was found to be greatly reduced in five mutant strains (*rad6*, *rad8*, *rev1*, *rev2*, and *rev3*), slightly reduced in one strain (*rad15*), and at wild type levels in the remainder (*rad1*, *rad2*, *rad4*, *rad9*, *rad18*, *rad50-57*). Oxygen enhancement ratios (OER) for mutagenesis are in the range of 2.0-3.0 at radiation doses giving close to 100% survival. These results are generally consistent with the existence of a single mutagenic repair pathway for radiation damage. Similarly,  $\gamma$ -ray survival studies with these same mutants are consistent with the three pathway models for radiation repair. Studies are currently being undertaken to more rigorously define this analysis with double mutant studies.

This work supported by NIH Grant GM 21858 and by ERDA at the University of Rochester ERDA project, and has been assigned Report No. UR-3490-1025.

**TH-AM-E7** ROLE OF HISTONE PROTEINS IN ULTRAVIOLET LIGHT-INDUCED PROTEIN-DNA ADDUCTS IN CHROMATIN. G.F. Strniste and S.C. Rall,\* Cellular and Molecular Biology Group, Los Alamos Scientific Laboratory, University of California, Los Alamos, New Mexico 87545

We have isolated and purified the nucleosome classes, monomer through tetramer, from nuclease-treated Chinese hamster cell nuclei. In agreement with the predicted model for chromatin substructure, our results indicate that, on the average, there exist two molecules each of histones H2A, H2B, H3, and H4 per chromatin subunit in each nucleosome class. The relative amount of histone H1 increases from monomer through tetramer. Using nucleosomes as a basic model system representing the protein:DNA interactions existing in chromatin, we have been investigating the role of the various histone proteins in the process of ultraviolet (uv) light (254 nm) induction of protein-DNA adducts. Using molecular sieve chromatography, the amount of protein eluting coincident with the DNA after salt dissociation (i.e., protein-DNA adducts) increases linearly with uv light fluence and is nearly invariable for the nucleosome classes tested (dimer through tetramer). Analysis of uv-irradiated nucleosomes on SDS-polyacrylamide gels shows a depletion of all five histones from their normal migrating positions in the gel. Histones H2A and H2B are removed more rapidly than are histones H3 and H4. In addition to protein-DNA adducts, at least 50% of the affected histones are induced to form other photoproducts, including protein-protein adducts and/or aggregates. One of the primary protein-protein photoproducts observed appears to be the H2A-H2B dimer. In the crosslinking process, irradiated nucleosomes differ from irradiated, sheared, soluble chromatin in that there is more histone involvement but less total protein linked, the latter result most likely being a consequence of the involvement of nonhistone protein in the crosslinking phenomenon observed in sheared, soluble chromatin. (This work was performed under the auspices of the USERDA.)

**TH-AM-E8** DNA REPAIR IN VITRO BY EXTRACTS OF ESCHERICHIA COLI. W. L. Carrier and W. E. Masker, Biology Division, Oak Ridge National Laboratory, Oak Ridge, TN 37830

Gently lysed extracts from various mutant strains of Escherichia coli have been examined for their ability to perform steps of excision repair in vitro. To overcome the inability of these extracts to efficiently carry out the incision step of the excision repair pathway an endonuclease from Micrococcus luteus was used to produce incisions at dimer sites in UV-irradiated DNA from T7 or PM2. This incised DNA was then used as an exogenous substrate to monitor the excision, resynthesis, and ligation steps of excision repair. Extracts prepared from wild type or recB strains were able to remove all pyrimidine dimers from incised DNA and to restore the DNA to its original molecular weight. This restoration was accompanied by an average incorporation of 17 nucleosides per pyrimidine dimer removed. The rate and extent of dimer excision by these extracts was determined by the number of sites sensitive to the M. luteus UV-specific endonuclease as well as by two-dimensional paper chromatography. The excision process, which is completed very rapidly by wild-type extracts, requires  $Mg^{++}$  and is stimulated by the presence of the four dNTP's; there is no apparent requirement for high concentrations of ATP. Extracts prepared from mutants deficient in the 5'→3' exonuclease of DNA polymerase I are only slightly deficient in in vitro dimer excision when compared to wild-type extracts. However, extracts from polA1 mutants show greatly reduced rates of dimer excision. Extracts prepared from uvrC mutants appear to perform normal excision of dimers from DNA previously incised with the UV-specific endonuclease. (Research supported by the U. S. Energy Research and Development Administration under contract with the Union Carbide Corporation.)

**TH-AM-E9** DNA REPAIR IN ESCHERICHIA COLI MUTANTS DEFICIENT IN THE 5'→3' EXONUCLEASE ACTIVITY OF DNA POLYMERASE I AND EXONUCLEASE VII. J. W. Chase\* and W. E. Masker, Department of Molecular Biology, Albert Einstein College of Medicine, Bronx, NY 10461 and Biology Division, Oak Ridge National Laboratory, Oak Ridge, TN 37830

A series of Escherichia coli strains deficient in one or both of two specific 5'→3' exonuclease activities [the 5'→3' exonuclease activity associated with DNA polymerase I (exonuclease VI) and exonuclease VII], both of which carry out thymine dimer excisions in vitro, has been constructed. These strains were examined for conditional lethality, sensitivity to ultraviolet (UV) and X-irradiation, postirradiation DNA degradation and ability to excise pyrimidine dimers. It was found that the combination of an xseA mutation (deficient in exonuclease VII) with mutations (polAex1, polAex2) temperature sensitive for exonuclease VI reduced the ability of these strains to survive incubation at elevated temperature (43°) beyond that previously observed for the polAex single mutants. The UV and X-ray sensitivity of the exonuclease VI deficient strains was not significantly increased by the addition of the xseA mutation. Mutants deficient in both enzymes are about as efficient as wild type strains at excising dimers produced by up to 40 J/m<sup>2</sup> UV. At higher doses strains containing only polAex mutations show reduced ability to excise dimers; however, the interpretation of dimer excision data at these doses is complicated by extreme postirradiation DNA degradation in these strains. The additional deficiency in the polAex xseA double mutant strains has no significant effect on either postirradiation DNA degradation or the apparent deficiency in dimer excision at high dose observed in polAex single mutants. (Research supported by the U. S. Energy Research and Development Administration under contract with the Union Carbide Corporation.)

**TH-AM-E10 DAMAGE AND REPAIR OF A NON-FREELY-SEDIMENTING DNA COMPONENT FOLLOWING LOW AND HIGH LET IRRADIATION AND HYPERTHERMIC PRETREATMENT OF CHO CELLS.** A. Cole and I. Kristal\*, Physics Dept., University of Texas System Cancer Center, Houston, Texas 77030

When CHO cells are lysed in sakosyl on top of 5 M NaCl neutral sucrose density gradients, about 35% of the native DNA sediments freely to produce a distinct peak at 160 S. The remainder of the DNA is found as a non-freely-sedimenting-fraction (NFSF) which remains in the lysis zone or is attached to the walls of the polyalomer centrifuge tubes. Pretreating the tubes with native or denatured DNA does not affect the subsequent attachment of the NFSF. Irradiation of cells before lysis with gamma or alpha doses of 1 to 25 kR produces double strand DNA breaks, expressed as a reduction in the S value of the peak, and increases the amount of freely sedimenting DNA from 35% to over 90% (i.e. the NFSF is reduced from 65% to less than 10%). Alpha particle irradiation appears to be 1.5 times more dose efficient than gamma irradiation for inducing both effects. If the irradiated cells are incubated at 37°C before lysis, the sedimentation properties tend to those for unirradiated controls, i.e., first, the peak positions return toward 160 S during a fifteen minute incubation period and, second, the NFSF returns toward 65% during a two hour incubation period. The second process is inhibited by alpha irradiation above 5 kR or gamma irradiation above 10 kR. Hyperthermic pretreatment of cells at 43°C for 45 minutes before irradiation does not affect the sensitivity for induction of DNA breaks or reduction of the NFSF but does inhibit the ability of the cell to restore these defects during the post-irradiation incubation. Supported in part by ERDA Contract AT-(40-1)-2832.

**TH-AM-E11 THE *dnaB* GENE PRODUCT: A COMPARISON OF ITS ROLE IN DNA POLYMERASE III-DIRECTED REPLICATIVE AND X-RAY-INDUCED REPAIR SYNTHESIS.** D. Billen and G.R. Hellermann\*, The University of Tennessee-Oak Ridge Graduate School of Biomedical Sciences, Oak Ridge, Tennessee 37830 and Biology Division, Oak Ridge National Laboratory, Oak Ridge, Tennessee 37830

In *Escherichia coli* *dnaB* mutants a temperature shift from 30°C to 42.5°C results in an abrupt cessation of replicative DNA synthesis, presumably due to inactivation of the *dnaB* gene product (Wechsler and Gross, Mol. Gen. Genet. 113, 273-284, 1971). As part of a study to understand the relationships between enzymes and proteins involved in DNA repair synthesis, we have investigated the role of *dnaB* gene product in X-ray-induced repair synthesis carried out by DNA polymerase III in toluene-treated bacteria. In *polA1 polB1* mutants of *E. coli* deficient in both DNA polymerases I and II activities, X-ray-induced DNA repair synthesis still occurs in toluene-permeabilized cells presumably carried out by DNA polymerase III (Billen and Hellermann, J. Bacteriol. 126, 785-793, 1976). This repair synthesis is ATP dependent. Using a *polA1 polB1 dnaB* mutant we have determined that the X-ray-induced, ATP-dependent DNA repair synthesis is, unlike semiconservative DNA synthesis, unaffected at the restrictive temperature. The *dnaB* gene product therefore appears necessary for DNA polymerase III-directed replicative synthesis but not DNA polymerase III-directed repair synthesis.

(This work supported in part by ERDA contract AT-(40-1)-4568 and ERDA under contract with the Union Carbide Corporation).

By acceptance of this article, the publisher or recipient acknowledges the right of the U.S. Government to retain a nonexclusive, royalty-free license in and to any copyright covering the article.

**TH-AM-E12 LOCALIZATION OF INHIBITION OF REPLICON INITIATION TO DAMAGED REGIONS OF DNA IN CULTURED MAMMALIAN CELLS.** L.F. Povirk\* and R.B. Painter, Laboratory of Radiobiology, University of California, San Francisco, California 94143

Treatment of synchronized S-phase CHO cells with 313 nm light inhibited initiation of replicons in DNA substituted with bromodeoxyuridine. Estimates of the cross-section for total DNA base damage imply that a single lesion suppressed initiation of several replicons. However, replication of unsubstituted DNA, occurring simultaneously in the same cells, was unaffected. These results suggest that this inhibition and probably a similar inhibition induced by ionizing radiation, may be mediated by conformational changes in localized regions of individual DNA molecules.

**TH-AM-E13 DNA REPAIR IN ARRESTED HUMAN DIPLOID FIBROBLAST CULTURES IRRADIATED WITH ULTRA-VIOLET LIGHT.** G. J. Kantor and D. R. Hull\*, Department of Biological Sciences, Wright State University, Dayton, Ohio 45431

Cultured human diploid fibroblasts arrested with respect to division by incubation in medium containing 0.5% fetal calf serum detach from the surface of a culture plate following irradiation with UV (254 nm). The fraction of cells that eventually detach is fluence and cell strain dependent. DNA-repair deficient cells (XP12BE) are more sensitive than DNA-repair proficient cells (WI-38). Survival curves determined by measuring the number of cells remaining attached at 10 days post-UV, a time at which no further cell loss is detected, have a shoulder at low fluences and  $D_{37}$  values of  $37 \text{ J/m}^2$  for WI-38 and  $5.5 \text{ J/m}^2$  for XP12BE. The detached cells are not viable as indicated by uptake of viable stains and unsuccessful attempts at cultivation. Results to be presented were obtained in a study of the nature of the UV-induced damage that cause arrested cells to detach. Dose-fractionation experiments indicate that a repair of UV-induced damage occurs in both cell strains. DNA-repair, as determined by excision of thymine dimers and occurrence of unscheduled DNA synthesis (UDS), was detected in UV-irradiated arrested populations of WI-38 and to a significantly lesser extent in arrested XP12BE populations. Hydroxyurea and caffeine have no effect on the extent of UDS. Inhibitors of protein synthesis (puromycin, cycloheximide and actinomycin D) also cause arrested cells to detach from the culture surface. These results are interpreted to mean that (1) DNA-repair through the repair synthesis step occurs in arrested HDF populations, (2) DNA-repair is required for the continued maintenance of irradiated arrested populations and (3) the action of UV leading to detachment is DNA damage that inhibits synthesis of proteins required for maintenance of the arrested state. (Supported by NIH Grant CA-16477).

**TH-AM-E14 CONTRIBUTION OF SECONDARY RADICALS TO INDIRECT ACTION OF RADIATION.** D. Becker\* and L.I. Grossweiner, Department of Physics, Illinois Institute of Technology and Department of Medical Physics, Michael Reese Medical Center, Chicago, Illinois 60616.

Hutchinson<sup>1</sup> has shown that the effective target volume of a spherical object of radius  $r_0$  for the attack of radicals generated in the external medium is given by:  

$$v = 4\pi r_0^2 q(1 + r_0/\rho)$$
 with  $\rho^2 = D/a$ , where  $D$  is the diffusion constant and  $a$  is the scavenging rate constant, respectively, and  $q$  is a kinetic parameter near unity. The extension to secondary radicals (primed quantities) generated by scavenging of the primary radicals (un-primed quantities) is:  $v' = v(k_d'/k_d)(q'/q)(g'/a')(1 + r_0/\rho' + \rho)/(1 + r_0/\rho)$  where  $k_d$  is the diffusion-limited rate constant and  $g'$  is the secondary radical generation rate. The overall radiation sensitivity for indirect action is given by:  $D_{37}^{-1} = G(nv + \eta v')$  with  $G$  the radical yield per unit dose and  $\eta$  the biological efficiency per radical hit. This analysis has been applied to the inactivation of T7 phage by 25 Mev electrons in the presence of radical scavenging solutes: inorganic anions, amino acids and sugars, and demonstrates complex secondary radical contributions. (Supported by NCI Grant CA-13307).  
 (1) Hutchinson, F. (1957). *Radiat. Res.* 7, 473.

**TH-AM-E15 INDUCED RADIORESISTANCE IN TWO STRAINS OF E. COLI AND TWO  $\lambda$  LYSOGENS OF THEM.** Ernest C. Pollard, and D. J. Fluke, Department of Zoology, Duke University and Biophysics Program, Penn. State University.

Cells of *E. coli* which are not *recA*<sup>-</sup> nor *lex*<sup>-</sup> show an induced radioresistance when pre-treated by inducing agents such as UV, ionizing radiation or naladixic acid. The experimental procedure used is to give the inducing dose, or fluence, incubate for 40 minutes, block further transcription with rifampin and then irradiate with graded doses of x-rays or  $\gamma$ -rays. Strains AB 1157 and AB 1886 (*uvrA*<sup>-</sup>) show a decrease in sensitivity of between two and fourfold with this treatment. When the  $\lambda$ -lysogen was investigated it was found that higher UV fluences were needed to induce  $\lambda$  so that it should have been possible to induce radioresistance without inducing many cells for  $\lambda$ . We found this not to be the case. Both AB 1157  $\lambda$  and AB 1886  $\lambda$  showed no induced radioresistance at all when UV was employed as the inducing agent. A small amount of radioresistance developed with  $\gamma$ -radiation as the inducing agent.

When the *ind*<sup>-</sup> lysogens AB 1157  $\lambda_{ts857}$  and AB 1886  $\lambda_{ts857}$  were studied there was nearly normal induced radioresistance. The repressors of normal  $\lambda$  have been found by Sussman and Ben-Zeev (1) to bind to single strand breaks in the DNA while those of the *ind*<sup>-</sup> do not. Our experiments thus suggest that the presence of  $\lambda$  repressors in the cell is somehow competitive for the inducing signal or some event subsequent to it. The *ind*<sup>-</sup> repressors do not so compete.

<sup>1</sup>R. Sussman and H. Ben-Zeev (1975). *PNAS* 72, 1973-1976.

**TH-AM-E16 RELATIVE RATES OF DNA REPAIR AND DEGRADATION IN NORMAL AND INDUCED CELLS OF *E. COLI*.** James C. Fugate\* and Ernest C. Pollard, Department of Biochemistry & Biophysics, The Pennsylvania State University, University Park, PA 16802

Strains of *E. coli* which are  $recA^+$  and  $lex^+$  show the phenomenon of induced inhibition of postirradiation DNA degradation (prd). Observations in alkaline sucrose gradients can be used to estimate the amount of repair of single strand breaks and the amount of DNA degradation in gamma-irradiated cells. By using rifampin to block transcription it is possible to compare the repair and degradation in cells which have been induced for inhibition of prd and those which have not. Cells of WU36-10 were used and given 17.5 J/m<sup>2</sup> UV to induce inhibition of prd. They were then either immediately treated with 50 µg/ml rifampin for 10 min, or allowed to develop inhibition of prd for 40 min and then treated with rifampin. The cells were then irradiated with <sup>60</sup>Co gamma rays and incubated for various times at 37°C before lysing onto a 5-18% alkaline sucrose gradient. It was apparent in non-induced cells that (a) the repair of single strand breaks was 90% complete in 5 min; (b) DNA degradation is much slower and is not complete at 30 min; and (c) repaired DNA can be degraded. In the induced cells the rate of repair was somewhat slower and the degradation drastically reduced. It is likely that the slower repair rate simply reflects the increased amount of repairable DNA with no change in the concentration of repair enzymes. (Supported by ERDA grant E(11-1)-2362.)

**TH-AM-E17 MICROWAVE IRRADIATION, BEHAVIORAL AND OCULAR EFFECTS ON RHESUS MONKEYS.** R. McAfee, L. Cazenavette\*, H. Shubert\*, J. May\*, S.T. Elder\*, and R. Gordon\*, Research Department, V.A. Hospital, New Orleans, La. 70146, School of Engineering and Department of Psychology, University of New Orleans, and Ophthalmology Department, Tulane University School of Medicine, New Orleans, La.

Four adult rhesus monkeys were irradiated with 9.3 GHz pulsed microwave radiation to determine if observable deleterious effects to the eye and nervous system are produced when irradiated at allegedly harmful power densities and times. The rhesus were trained to lever press for a 0.2 ml squirt of orange drink from a plastic tube delivered on a 20% variable schedule. During a 20-minute session, the monkeys were allowed to respond for 5 minutes without being irradiated and were then irradiated over the face and eyes when drinking from the plastic tube. The irradiation session lasted 15 minutes. The rhesus could cease lever pressing and withdraw from the radiation if it desired to do so. The lever press rate for the unirradiated 5 minutes was compared with that during the last 5 minutes. Infrared irradiation sessions were interspersed with microwave sessions for comparison. Responses were suppressed as the dose of infrared radiation increased but not when the microwave irradiation intensity increased up to 495 mw/cm<sup>2</sup> for 15 minutes. Thus, behavioral effects of microwave irradiation (on motivation and activity directed toward obtaining a reward) were not seen and ocular effects such as lenticular opacity formation were not observed after two years of observation.

**TH-AM-F1 A FLUORESCENCE ENERGY TRANSFER STUDY ON THE DISTANCE BETWEEN AN ESSENTIAL SULFHYDRYL GROUP AND THE 8-ANILINO-1-NAPHTHALENESULFONATE SITE ON BACTERIAL LUCIFERASE.**

S.-C. Tu and J.W. Hastings, Biological Laboratories, Harvard University, Cambridge, MA 02138

Bacterial luciferase catalyzes the bioluminescent oxidation of FMNH<sub>2</sub> and a long chain aldehyde by O<sub>2</sub>. Delineation of the structure of luciferase active center is of fundamental importance for better understanding of the mechanism by which chemical energy is converted to light. Previous chemical modification studies showed that an essential sulfhydryl group is at or near the luciferase active center. It is also known that 8-anilino-1-naphthalene-sulfonate (ANS) binds to luciferase with an 1:1 molar ratio, and functions as an inhibitor competitive with FMNH<sub>2</sub>. In the experiments reported here, fluorescence energy transfer is employed to determine the distance between the ANS site and the essential sulfhydryl residue. Luciferase was stoichiometrically labeled with a fluorescent probe by treatment with an equi-molar quantity of N-(p-(2-benzoxazolyl)phenyl)maleimide, yielding enzyme with a N-(p-(2-benzoxazolyl)phenyl)succinimido group (NBPS) at the reactive cysteinyl residue. The labeled enzyme is inactive in bioluminescence emission but binds ANS with an unaltered K<sub>d</sub> (2.5 × 10<sup>-5</sup> M at 23°, pH 7). The NBPS group exhibits a fluorescence quantum yield of 0.07 and an emission (λ<sub>max</sub>, 360 nm) overlapping well with the absorption (λ<sub>max</sub>, 370 nm) of luciferase-bound ANS (ANS<sub>b</sub>). Using the NBPS group as the fluorescence donor and ANS<sub>b</sub> as the acceptor, the overlap integral (J) and critical transfer distance (R<sub>0</sub>) are calculated to be 8.7 × 10<sup>-15</sup> cm<sup>3</sup> M<sup>-1</sup> and 21 Å, respectively. Fluorescence energy transfer efficiencies were measured using the labeled enzyme with different amounts of bound ANS. Calculations based on the amount of ANS<sub>b</sub> gave a transfer efficiency of 65(± 8)%, corresponding to a distance of 19(± 1) Å between the NBPS-labeled cysteinyl residue and the ANS site on luciferase.

**TH-AM-F2 LIGHT EMISSION FROM A LUCIFERASE-FLAVIN INTERMEDIATE IN THE ABSENCE OF OXYGEN.**

J.E. Becvar, S.-C. Tu, and J.W. Hastings, The Biological Laboratories, Harvard University, Cambridge, MA 02138

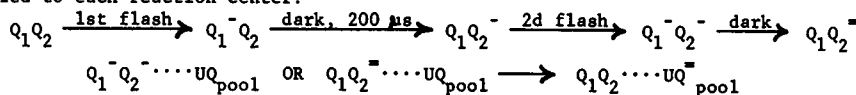
Bacterial bioluminescence results from the luciferase mediated oxidation of reduced flavin mononucleotide and aliphatic aldehyde by molecular oxygen. A mechanism has been proposed which involves the reaction of a long-lived flavoenzyme intermediate (designated II and postulated to be a luciferase:4a-hydroperoxy flavin intermediate) with aldehyde, to yield an electronically excited product which subsequently emits light. In the absence of aldehyde, II decomposes with at least a thousand times less luminescence. A prediction from the proposed mechanism is that once intermediate II is formed, molecular oxygen is no longer required for light emission. We have now verified that this is the case. When aliquots of II at 0° are made anaerobic and then injected into oxygen free aldehyde solutions in 0.1 M phosphate buffer, pH 7, at 25°, the resulting yield of light is the same as was obtained in parallel experiments under aerobic conditions. Moreover, the kinetic properties of the emission (maximal emission intensity and rate of light decay) are identical under aerobic and anaerobic conditions. Our results also indicate that the absence of free molecular oxygen does not seem to affect the rate of decomposition of II. Anaerobicity in all solutions was achieved using glucose/glucose oxidase and was verified in control experiments by a sensitive oxygen detecting system utilizing the bacterial luciferase reaction itself.

**TH-AM-F3 MOLECULAR ORBITAL CALCULATIONS ON THE CONVERSION OF THE VISUAL PIGMENT CHROMOPHORE FROM AN EVEN TO ODD π-SYSTEM. Paul Blatz and Heme Navangul\*, Chemistry Department, University of Missouri-Kansas City, Kansas City, Missouri 64110**

PPP-molecular orbital calculations are made on the even, twelve p-orbital chromophoric molecule N-retinylidene-n-butylammonium cation. The even π-system is gradually converted in an odd π-system by continuously increasing the positive charge on nitrogen (Z<sub>p</sub>) that is used to polarize the π-electrons. In the calculations, the increase in Z<sub>p</sub> is accounted for by continuously adjusting the orbital occupancy and the coulomb integral α<sub>N</sub>. As Z<sub>p</sub> changes, the following output parameters are examined: excitation energy, wavefunction geometry, eigenvalues of wavefunctions, bond order, electron density and resonance energy. The output parameters are completely consistent with conversion from even to odd as the value of Z<sub>p</sub> goes to unity. The eigenvectors reveal that the first π-orbital is transformed from a molecular orbital to an atomic orbital centered over nitrogen. Also the first unoccupied MO is transformed from antibonding to nonbonding. The overall changes in the π-system are related to the chromophoric molecule in visual pigments.

**TH-AM-F4 ELECTRON TRANSFER BETWEEN PRIMARY AND SECONDARY ELECTRON ACCEPTORS IN REACTION CENTERS FROM RHODOPSEUDOMONAS SPHAEROIDES.** A. Vermeglio\* and R. K. Clayton, Division of Biological Sciences, Cornell University, Ithaca, New York 14853.

When reaction centers from *R. sphaeroides* are exposed to a sequence of brief (single turnover) flashes of light, they show oscillating absorbance changes characteristic of the formation of ubisemiquinone on odd-numbered flashes and its conversion to fully reduced ubiquinone (UQ) on even flashes. A pattern of multiple oscillations (with damping) is seen only if excess electron donor and UQ have been added. In the absence of exogenous UQ a single oscillation is observed. Oscillations are suppressed by orthophenanthroline. This behavior is explained by a model in which two molecules of UQ ( $Q_1$  and  $Q_2$ ) are coupled to each reaction center:



In this model  $Q_1$  receives an electron from bacteriochlorophyll in the photochemical act. The oxidized bacteriochlorophyll is rereduced by the exogenous donor. Exogenous UQ can be reduced in a two-electron transfer from  $Q_2^-$  or perhaps from  $Q_1^- Q_2^-$ . Reduction of either  $Q_1$  or  $Q_2$  to the semiquinone is attended by shifts of the absorption bands of bacteriochlorophyll and bacteriopheophytin in the reaction center, and the spectra of these shifts are different for  $Q_1$  and  $Q_2$ . Electron transfer from  $Q_1$  to  $Q_2$  can therefore be observed by the change in band shift spectra; the half-time for this transfer is 200  $\mu\text{s}$ .

**TH-AM-F5 ALLOPHYCOCYANIN: THE FRACTIONATION OF DISTINCT FORMS FROM THE BLUE-GREEN ALGA NOSTOC SP.** by Burke K. Zimmerman, Barbara A. Zilinskas\*\* and Elisabeth Gantt\*, Radiation Biology Laboratory, Smithsonian Institution, Rockville, Md. 20852 and Dept. Biochemistry and Microbiology, Rutgers University, New Brunswick, N.J. 08703\*

Light energy absorbed by intact phycobilisomes of the blue-green alga *Nostoc sp.* is transferred with high efficiency to a pigment with a fluorescence emission peak of 675-680 nm. This property is believed to reflect the efficient transfer of light energy absorbed by phycobilisomes in vivo to chlorophyll a. Allophycocyanin, derived from *Nostoc* phycobilisomes, was fractionated by calcium phosphate gel chromatography and zone sedimentation in the preparative ultracentrifuge to yield three well-resolved distinct pigments and traces of a fourth. The properties of these pigments are shown in the following table:

Form	S20,w	Absorption $\lambda_{\text{max}}$	$A_{620}$ $A_{\lambda_{\text{max}}}$	$A_{680}$ $A_{\lambda_{\text{max}}}$	Fluorescence $\lambda_{\text{max}}(23^\circ\text{C})$	Rel. Amount (by $A_{\lambda_{\text{max}}}$ )
I	6.0 $\pm$ .1	654	.39	.35	678 $\pm$ 2	14-22%
II	5.0 $\pm$ .1	650	.63	.03	659 $\pm$ 2	40-50%
III	5.3 $\pm$ .2	650	.45	.03	662 $\pm$ 2	30-40%
B <sup>a</sup>	4.9 $\pm$ .2	618 & 671 <sup>a</sup>	-	-	678 $\pm$ 2	<5%

The pigment form designated I as well as the minor pigment, probably comparable to allophycocyanin B described by Glazer and Bryant<sup>a</sup>, both exhibit fluorescence emission at 678 nm, the same as that of intact phycobilisomes. However, allophycocyanin form I is distinct from the minor component by a characteristic absorption spectrum, a larger sedimentation constant, and it is considerably more abundant, accounting for about 20% of the total.

<sup>a</sup>Arch. Mikrobiol. 104, 15-22 (1975). Supported in part by ERDA contract E(40-1)-4310.

**TH-AM-F6 FLUORESCENCE QUANTUM YIELDS AND ENERGY MIGRATION IN PHYCIBILISOMES WITH DIFFERENT PHYCIBILIPROTEIN COMPOSITION.** J. Grabowski\* and E. Gantt\*, (Introduced by W. Shropshire, Jr.), Radiation Biology Laboratory, Smithsonian Institution, Rockville, Md. 20852

Quantum yield and fluorescence polarization determinations on phycobilisomes and their constituent phycobiliproteins show that phycobilisomes are energetically effective macromolecular structures. Energy migration within the phycobilisome to allophycocyanin, the longest wavelength absorbing and emitting phycobiliprotein, was indicated by the predominant allophycocyanin fluorescence emission which was independent of the phycobiliprotein being excited. The high efficiency of the energy migration inside the phycobilisome was reflected by the low polarized fluorescence. Excitation of phycobilisomes in their major absorption region of 500-650 nm resulted in degrees of fluorescence polarization between +0.02 and -0.02, whereas in isolated phycobiliproteins the values were 2 to 8 times greater. Furthermore, 95-99% of the excitation energy of phycoerythrin was transferred to phycocyanin and allophycocyanin as determined from comparisons of fluorescence spectra of intact and dissociated phycobilisomes. The quantum fluorescence yield of allophycocyanin was 0.68, which is very similar to that of intact phycobilisomes. Phycobilisomes isolated from *Nostoc sp.* (a blue-green alga) had a quantum yield of 0.65, and those isolated from *Porphyridium cruentum* (a red alga) had one of 0.55. The quantum yield remained essentially unchanged when the ratios of the constituent phycobiliproteins were varied by growing cells at different wavelengths. In *Nostoc sp.*, which showed a striking adaptation to different wavelengths, the phycobilisome quantum yield only varied from 0.65 to 0.60. The results confirm that the efficiency of energy transfer is dependent on the close structural association of the phycobiliproteins within the phycobilisome, and suggest that variation in pigment composition has a relatively small effect on the efficiency in the same species.

TH-AM-F7 TWO-PHOTON PROCESSES IN PHOTOSYNTHETIC SYSTEMS. M. Chu Kung\* and D. DeVault, Johnson Research Foundation, Dept. of Biochemistry and Biophysics, Univ. of Penna., Philadelphia, PA 19174.

Excitation of the antenna system of the photosynthetic bacterium, *R. sphaeroides*, mutants Ga and R-26, with laser pulses of either 694nm or 868nm produces a weak fluorescence with peaks at 440nm, 530nm, and 600nm. Quantum yield for the 440nm peak is roughly  $1.3 \times 10^{-9}$  and for the 600nm peak,  $2.3 \times 10^{-9}$  photons emitted per photon absorbed. The 530nm peak, being lower but broader than the other two has a similar quantum yield. The intensity of excitation was up to 0.7 photons absorbed per BChl molecule per nsec for a 25 nsec pulse. *R. viridis*, which contains BChl b absorbing out to 1010nm, gave a smaller peak at 440nm and a peak at 530nm.

It is proposed that singlet-singlet annihilation promotes an exciton to a state,  $S_n$ , with twice the excitation energy of the  $S_1$  state and that the radiation results as  $S_n$  decays thru several intermediate levels. Assuming the processes:  $S_0 \xrightarrow{I} S_1$ ;  $S_1 \xrightarrow{k_1} S_0$ ;  $2S_1 \xrightarrow{k_2} S_n + S_0$ ; and  $S_n \rightarrow S_0 + \text{Radiation} + \text{Heat}$ ; and that the conc. of BChl in the membrane is 60mM, one calculates from the upward concavity of the dependence on excitation intensity that  $k_2$  is  $10^{10}$  to  $10^{11} \text{ M}^{-1} \text{ sec}^{-1}$  if  $k_1$  is  $10^9 \text{ sec}^{-1}$ , or  $10^{12}$  to  $10^{13} \text{ M}^{-1} \text{ sec}^{-1}$  if  $k_1$  is  $10^{10} \text{ sec}^{-1}$ .

This work was supported by NSF Grant PCM76-15724.

TH-AM-F8 MAGNETIC FIELD EFFECTS ON BIRADICAL INTERMEDIATES IN BACTERIAL PHOTOSYNTHESIS R. E. Blankenship\*, T. J. Schaafsma\*, W. W. Parson\*, Intr. by M. P. Gordon, Department of Biochemistry, University of Washington, Seattle, WA, 98195

The room-temperature quantum yield of flash-induced bacteriochlorophyll triplet formation in chemically reduced reaction centers of *Rps. sphaeroides* strain R-26 is decreased by 40% upon application of a 2 Kgauss magnetic field. A 50% decrease is observed in carotenoid triplet quantum yield in reaction centers of strain 2.4.1. The field dependence of the effect shows a monotonic decrease saturating at about 1 Kgauss. No magnetic field effect is observed on bacteriochlorophyll triplet yield *in vitro* or on P870+ formation in reaction centers at moderate potential. The effect of the field becomes less at lower temperature, (15% at 80°K) where the triplet yield is higher, in agreement with predictions of a simple kinetic theory. The existence of the magnetic field effect is taken to be strong evidence in favor of the biradical model of bacterial photosynthesis. The sign of the magnetic field effect indicates, in agreement with psec absorption measurements, that the biradical is born in a singlet state. Local magnetic field differences evidently induce singlet-triplet mixing in the biradical, and the triplet states observed in reduced reaction centers arise from biradicals with triplet character, rather than via the traditional route of intramolecular intersystem crossing. The magnetic field is interpreted as affecting triplet yields by decreasing the number of biradical triplet states in equilibrium with the singlet state, from three at zero field to one at high field. Equilibration between singlet and triplet levels of the biradical is concluded to be rapid at both zero and high fields.

TH-AM-F9 THE EFFECTS OF DBMIB ON PRIMARY PHOTOCHEMISTRY IN RHODOSPIRILLUM RUBRUM. Charles L. Bering, Jr. and Paul A. Loach, Department of Biochemistry and Molecular Biology, Northwestern University, Evanston, IL 60201.

Dibromothymoquinone (DBMIB) has been widely used as a plastoquinone antagonist in chloroplasts. Several workers have reported that it also inhibits ubiquinone (UQ) functions. Since UQ has been implicated as having a role in the primary photochemistry of purple nonsulfur bacteria, we have examined the effects of DBMIB on chromatophores of *Rhodospirillum rubrum*. With continuous red illumination, we observed a pronounced decrease in efficiency of  $P865^{++}$  formation. Using a short (5  $\mu\text{sec}$ ) exciting pulse, we observed that DBMIB inhibits  $P865^{++}$  formation as measured by absorbance changes of the trap bacteriochlorophyll at 430 and 605 nm. Half maximal inhibition was obtained at a DBMIB/ $P865$  ratio at about 25. The decay kinetics were also significantly slowed with DBMIB. The inhibition of the absorbance change was reversed upon addition of UQ. With a five-fold excess of UQ to DBMIB we were able to restore the  $\Delta A_{430}$  to about 75% of the untreated sample. Previous results from our laboratory indicated that two UQ pools exist in chromatophores - a tightly-bound pool, required for phototrap activity, and a loosely-bound pool (Morrison, et al. Biophys. J. (1976) 16, F-PM-D5). We were able to determine the concentration of UQ in both pools using cells grown on  $^{14}\text{C}$ -p-hydroxybenzoic acid, which labels quinones specifically. With labelled chromatophores, we observed displacement of approximately one-half of the tightly-bound UQ, which becomes extractable with the loose pool. Our results show that DBMIB displaces UQ, and may be competitively binding at the level of the primary electron acceptor.

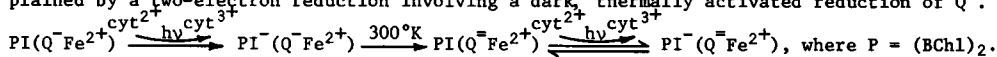


**TH-AM-F10 THE CONTROL OF REACTION CENTER BACTERIOCHLOROPHYLL PHOTO-OXIDATION.** T.L. Netzel\*, D.M. Tiede\*, R.C. Prince\*, P.L. Dutton\*, and P.M. Rentzepis, Bell Laboratories, Murray Hill, NJ 07974 and Johnson Research Foundation, U. of Pennsylvania, Phila., PA 19174.

The photo-oxidation of the reaction center bacteriochlorophyll dimer or special pair (BChl)<sub>2</sub> has been monitored at 1235 nm in *C. vinosum* and at 1310 nm in *Rps. viridis*. In both species the photo-oxidation is complete within 10 ps of a flash of light. The reaction proceeds unimpeded at low temperatures and regardless of the prior state of reduction of the traditional "primary" electron acceptor, a quinone-iron complex. Thus the requirement for an intermediary electron carrier (I), previously established in this way in *Rps. sphaeroides* is clearly a more general phenomenon. This intermediary redox carrier, which involves bacteriopheophytin (BPh) and has been previously characterized by EPR and optical spectroscopy, has been examined here for its role as the direct electron acceptor from the photo-excited reaction center (BChl)<sub>2</sub>. To accomplish this, the extent of light-induced (BChl)<sub>2</sub> oxidation has been measured directly by the picosecond response of the infrared bands, and indirectly by EPR assay of the triplet/biradical, as a function of the state of reduction of the I/I<sup>•</sup> couple (measured by EPR) prior to flash activation. Two independent methods of obtaining I in a stably reduced form were used; chemical equilibrium reduction, and photochemical reduction. In both cases the results demonstrate that the intermediary carrier, which we have designated I and involves BPh, alone governs the capability for reaction center (BChl)<sub>2</sub> photo-oxidation, and as such I appears to be the immediate and sole electron acceptor (in the ground state) from the light-excited (BChl)<sub>2</sub>. Supported by NSF PCM 76-14209.

**TH-AM-F11 ON THE TRAPPING OF THE TRANSIENT ACCEPTOR IN REACTION CENTERS (RCs) OF R. SPHAEROIDES R-26.**† M.Y. Okamura, R.A. Isaacson\*, G. Feher, Phys. Dept., U.C.S.D., La Jolla, CA 92093.

The proposed<sup>1,2</sup> transient acceptor, I<sup>-</sup>, in bacterial photosynthesis has recently been stabilized by photoreduction at low potential.<sup>3,4</sup> We have done this with RCs of *R. sphaeroides* illuminated at 300°K (0.2mM horse heart cyt c, 2mM Na<sub>2</sub>S<sub>2</sub>O<sub>4</sub>, 0.1% Triton X-100, 50mM Tris pH 8). The optical absorption changes were characteristic of I<sup>-</sup>.<sup>3,4</sup> However, the EPR spectrum (4°K) differed from that observed earlier.<sup>4</sup> In RCs, a single narrow resonance was observed, whereas in *C. vinosum* illuminated at 200°K two additional broad lines were obtained.<sup>4</sup> The explanation of this difference is suggested by the observed lag in the buildup of the optical and EPR changes during the initial illumination of RCs. During this lag period, the EPR spectrum due to the primary acceptor (g=1.8) decreased irreversibly. The optical and EPR changes due to I<sup>-</sup> were reversible and showed no lag on subsequent illuminations. Quinone-free RCs gave similar optical and EPR changes but showed no initial lag. These results are explained by a two-electron reduction involving a dark, thermally activated reduction of Q<sup>-</sup>.



The doublet EPR structure results from the magnetic interaction of I<sup>-</sup> and Q<sup>-</sup>Fe<sup>2+</sup>, whereas the narrow EPR line is due to I<sup>-</sup>Q<sup>-</sup>Fe<sup>2+</sup>. The narrowness of the I<sup>-</sup>-line (in comparison to that obtained from Q<sup>-</sup>Fe<sup>2+</sup>) indicates that I<sup>-</sup> is further removed from Fe<sup>2+</sup> than the quinone Q.

<sup>1</sup>Rockley, et al., PNAS (1975) 72, 2251. <sup>2</sup>Fajer, et al., PNAS (1975) 72, 4956. <sup>3</sup>Shuvalov, et al., Biochim. Biophys. Acta (1976) 440, 587. <sup>4</sup>Tiede, et al., FEBS Letters (1976) 65, 301.

†Work supported by NSF Grant BMS-74-21413 and NIH Grant GM-13191.

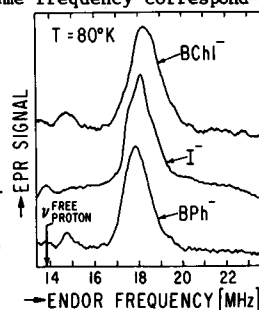
**TH-AM-F12 COMPARISON OF EPR AND ENDOR SPECTRA OF THE TRANSIENT ACCEPTOR IN REACTION CENTERS OF R. SPHAEROIDES WITH THOSE OF BACTERIOCHLOROPHYLL AND BACTERIOPHEOPHYTIN RADICALS.**† G. Feher, R.A. Isaacson\*, M.Y. Okamura, Physics Dept., U.C.S.D., La Jolla, Calif. 92093.

The transient acceptor, I<sup>-</sup>, was photoinduced in RCs of *R. sphaeroides* R-26 as described by Okamura, et al. in the previous abstract. Its EPR characteristics are compared at 80°K and 9 GHz with those obtained from BChl<sup>-</sup> and BPh<sup>-</sup> prepared according to Fajer, et al.<sup>1</sup> by photo-oxidation in pyridine and Na<sub>2</sub>S. The results are summarized together with those obtained from the donor, P<sup>+</sup>, and BChl<sup>+</sup> (see Table). The ENDOR spectra of I<sup>-</sup>, BChl<sup>-</sup>, and BPh<sup>-</sup> all show a strong transition at approximately the same frequency corresponding to a hyperfine interaction of 8-9MHz (see Fig.). From a comparison of the optical spectra of I<sup>-</sup> with those obtained from model compounds, it has been suggested that I<sup>-</sup> is a tetrapyrrole anion (for a review, see ref. 1). The EPR and

ENDOR results corroborate this assignment and in addition provide strong evidence that I<sup>-</sup> (unlike P<sup>+</sup>) is a monomeric tetrapyrrole anion. More detailed experiments will, however, be required to differentiate between BChl<sup>-</sup> and BPh<sup>-</sup>.

<sup>1</sup>J. Fajer, M.S. Davis, D.C. Brune, L.D. Spaulding, D.C. Borg, & A. Forman, Brookhaven Symp. in Biol. #28, June, 1976, and references therein.

†Work supported by NSF Grant BMS 74-21413 and NIH Grant GM-13191.



TH-AM-F13 ENDOR AND ESR CHARACTERISTICS OF BACTERIOPHEOPHYTIN AND BACTERIOCHLOROPHYLL ANION RADICALS. J. Fajer,\* M. S. Davis,\* and A. Forman,\* (Intr. by J. M. Olson), Brookhaven National Laboratory, Upton, New York 11973.

Anion radicals of bacteriopheophytin (BPh) and bacteriochlorophyll (BChl) a and b have been prepared by chemical, electrolytic and photolytic reduction and their ESR parameters obtained in fluid and frozen solutions.

	g value	$\Delta H$ , $\dagger$ G ( $^{\circ}$ K)	ENDOR, G, ( $^{\circ}$ K)
BPh a <sup>-</sup>	2.0030 $\pm$ 0.0002	12.2-13 (110 $^{\circ}$ )	3.1 (100 $^{\circ}$ ); 3.0, 2.5 (273 $^{\circ}$ )
BChl a <sup>-</sup>	2.0028 - 2.0032	12.7-13 (130 $^{\circ}$ )	3.1 (~4 $^{\circ}$ ); 3.2 (80 $^{\circ}$ ); 3.3, 3.1, 2.5, 2.0 (240 $^{\circ}$ )
BPh b <sup>-</sup>	2.0033 $\pm$ 0.0002	12.2-13 (110 $^{\circ}$ )	3.1 (110 $^{\circ}$ ); 2.9, 2.5 (240 $^{\circ}$ )
BChl b <sup>-</sup>	2.0033 $\pm$ 0.0002	12.8-13 (130 $^{\circ}$ )	3.0 (110 $^{\circ}$ )

$\dagger$ (at 0.01 and 0.1mW)

The radicals exhibit partially resolved ESR spectra in solutions which can be satisfactorily simulated using a combination of ENDOR data, deuterations, model compounds and molecular orbital calculations to assign specific sites of unpaired spin densities. BPh and possibly BChl are postulated to act as transient electron acceptors in the primary charge separation of bacterial photosynthesis. The g values, linewidths ( $\Delta H$ ) and low temperature ENDOR results do not differ enough to provide the criteria necessary to distinguish between anion radicals of BPh and BChl in vivo.

This work was performed under the auspices of the U.S. Energy Research and Development Administration.

**TH-AM-G1 DONNAN EQUILIBRIA AND MEMBRANE POTENTIALS IN HUMAN RED BLOOD CELLS: A CALIBRATION OF THE FLUORESCENT PROBE, DiS-C<sub>3</sub>-(5).** Jeffrey C. Freedman\* and Joseph F. Hoffman, Department of Physiology, Yale University School of Medicine, New Haven, Conn. 06510.

Human red blood cells suspended in isotonic media and rendered cation permeable with nystatin could be maintained at their normal volume with 37 mM sucrose. These cells showed a very slight pH dependence of water content, in accordance with the Jacobs-Stewart equations as modified by including the osmotic coefficient of hemoglobin. Measurements of equilibrium cation ratios enabled calculation of Donnan potentials, which decreased by 10 mV between pH 6.5 and 8.5. Simultaneous measurements of pH and fluorescence of cell suspensions with DiS-C<sub>3</sub>-(5) during alternate additions of acid and base showed reversibility of the dye as an indicator of equilibrium membrane potentials. The calibration factor was 7-8% change in fluorescence per millivolt, much larger than observed in experiments where internal pH does not vary. In this study, erratic xenon arc wander noise was electromagnetically stabilized and scattered light interference was reduced to 0.5% of the signal with filters, enabling stable measurements with cells of changing volumes. Split beam absorption spectra of dye in the presence of cells versus cells alone appeared to exhibit an enhanced dimer absorption peak at 595 nm compared to dye in aqueous buffer. Normal untreated cells at decreasing external potassium, K<sub>o</sub>, showed, after valinomycin addition, decreases in monomer absorption, M, at 658 nm and corresponding increases in dimer absorption, D, which were consistent with a potential dependent dye partition with dimerization of cell associated dye. Dual wavelength absorption measurements showed that a function,  $\ln (M/\sqrt{D})$ , which is linear with membrane potential in certain monomer-dimer models, increased nonlinearly with  $\ln K_o$  between 1 and 150 mM. (Supported by USPHS Grants HL 09906, AM 17433, and GM 00167.)

**TH-AM-G2 CHARACTERISTICS OF CATION AND ANION MOVEMENTS IN TWO SUB-GROUPS OF DOG RED BLOOD CELLS.** Vincent Castranova and Joseph F. Hoffman, Dept. of Physiology, Yale University School of Medicine, New Haven, Conn. 06510.

After incubation of dog red blood cells in isotonic KCl (pH 7.4) for one hour at 37°C, the cells can be separated by centrifugation into two sub-groups, i.e., an upper layer of swollen cells and a lower more dense layer of slightly shrunken cells (Davson, 1942). These two groups of red cells are first returned to normal cell volume by incubation in an isotonic high Na-low K medium (pH 7.4). Then the rate constants for the efflux of sodium, potassium, and sulfate are measured at 37°C in each of these two cell sub-groups. Na efflux and the SO<sub>4</sub> equilibrium exchange flux are larger in cells derived from the lower layer while K efflux is larger in those cells harvested from the upper layer. Cation permeability in the normal population of dog red cells (before separation) is very dependent on cell volume, i.e., Na permeability is largest in shrunken cells and K permeability is largest in swollen cells. This property is not common to both sub-groups of dog red cells. Rather, the lower layer of cells shows far greater volume dependence of Na movement while the increase in K permeability with cell swelling is mainly a property of the upper layer of cells. These distinctions in transport are not due to differences in cell age. It is suggested that the reciprocal dependence of Na and K permeability on cell volume in the normal population of dog red blood cells may reflect the summed contribution of these two sub-groups of cells. (Supported by USPHS grants HL 09906 and AM 17433 and USPHS Fellowship HL 00400.)

**TH-AM-G3 Carboxylic Ionophore-Induced Cation Transport in Red Cells** B.C. Pressman and R. Greenwald\*. Department of Pharmacology, University of Miami, Miami, Florida 33152.

Carboxylic ionophores, selective for transporting monovalent cations (Na<sup>+</sup>, K<sup>+</sup>, H<sup>+</sup>), each show different degrees of divergence between their threshold doses for dilating coronary arteries and increasing cardiac contractility. (Ann. N.Y. Acad. Sci. 264,373). Our earlier assumption that these effects derive from the common ability of these agents to induce intracellular increase in Na<sup>+</sup>, in exchange for plasma K<sup>+</sup>, does not account for their pharmacological non-equivalence. Accordingly we examined the ability of various ionophores to shift intracellular pH in a model system of fresh, washed, human red cells suspended in a protein-free, buffered medium of 140 mM NaCl-5 mM KCl. Rates of extracellular  $\Delta$  pH and  $\Delta$  K<sup>+</sup> were measured with ion selective electrodes, correcting for the Na<sup>+</sup> sensitivity of the K<sup>+</sup> electrode. Rates of  $\Delta$  Na<sup>+</sup> were calculated from the algebraic sums of rates of  $\Delta$  pH and  $\Delta$  K<sup>+</sup>. The observed rates of pH shifts correlated with the known K<sup>+</sup> and Na<sup>+</sup> equilibrium affinities of the test ionophores. The ionophores could be grouped as: (1) inducing intracellular pH rise, K<sup>+</sup> affinity > Na<sup>+</sup> (X-537A, nigericin, X-206); (2) inducing little pH shift, K<sup>+</sup> affinity  $\approx$  Na<sup>+</sup> (lysocellin, A-204, Ro 21-6150); (3) inducing intracellular pH fall, K<sup>+</sup> affinity < Na<sup>+</sup> (monensin, dianemycin). We conclude that alteration of intracellular pH may be one of the components of the pharmacological effects of carboxylic ionophores. Supported by NIH Grant HL-16117.

**TH-AM-G4 A RESOLUTION OF THE MECHANISM OF GALACTOSE TRANSPORT IN HUMAN ERYTHROCYTES.**

H. Ginsburg and S. Yeroushalmi\*, Department of Biochemistry, University of Virginia School of Medicine, Charlottesville, Va. 22901, and Biophysics Group, Institute of Life Sciences, The Hebrew University, Jerusalem, Israel.

The kinetic properties of the mediated transport of galactose in human erythrocytes is investigated. Different methodological procedures are used to acquire a complete kinetic description of the system. Under zero-trans conditions, the uptake of galactose is mediated by two distinctly different carriers (defined as  $\alpha$  and  $\beta$ ) having similar maximal velocities but significantly different Michaelis constants:  $K_{01}^{zt} = 12.7 \pm 1.1$  mM;  $K_{01}^{zt} = 39.2 \pm 1.7$  mM·min<sup>-1</sup>;  $K_{01}^{zt} = 81.5 \pm 30.7$  mM;  $V_{01}^{zt} = 43.5 \pm 27.8$  mM·min<sup>-1</sup>. The zero-trans efflux displays only one carrier with the following kinetic parameters:  $K_{01}^{zt} = 74.4 \pm 23.9$  mM;  $V_{01}^{zt} = 241 \pm 65$  mM·min<sup>-1</sup> and so in the equilibrium exchange unidirectional flux:  $K^{ee} = 145.8 \pm 31.6$  mM;  $v^{ee} = 521.3 \pm 112.8$  mM·min<sup>-1</sup> of which 17% is contributed by the  $\beta$ -carrier which has a similar calculated Michaelis constant. The data of the  $\alpha$ -carrier are analyzed in terms of the simple carrier model as formulated by Lieb & Stein (Biochim. Biophys. Acta 373 (1974) 178). Using this model and the above kinetic parameters, a Michaelis constant for infinite-cis uptake can be derived, in full accord with the experimentally derived value of 21-25 mM. Application of several rejection criteria developed for the simple carrier using the kinetic parameters of the  $\alpha$ -carrier, failed to indicate lack of fitness of the model in the present case. From the analysis of kinetic data it is inferred that the movement of the unloaded carrier is the rate limiting step in the transport of galactose. The present work provides evidence that the transport of galactose is mediated by two asymmetric carriers operating in antiparallel fashion. The  $\beta$ -carriers comprise at most 15% of the total carrier population.

**TH-AM-G5 POTENTIAL ROLE OF VINBLASTINE-SENSITIVE ELEMENTS IN SUGAR TRANSPORT REGULATION.**

C.F. Whitfield, Physiology Department, The Pennsylvania State University, M.S. Hershey Medical Center, Hershey, Pennsylvania 17033.

Vinblastine is known to bind to microtubular proteins and cause their aggregation in the region near the cell membrane, and to cause preprecipitation of isolated contractile-like proteins, such as spectrin, *in vitro*. Recent reports from several laboratories suggest that vinblastine can alter erythrocyte shape and permeability to sodium. Therefore, the effect of vinblastine on sugar entry was investigated, using avian erythrocytes which have a regulated rate of sugar entry. Vinblastine sulfate (VBS) ( $1.5 \times 10^{-3}$  M) stimulated 3-O-methylglucose entry two fold. The activity coefficient of the carrier,  $F_s$ , increased from  $7.25 \pm 0.44$  to  $14.11 \pm 1.06$   $\mu$ l/g·min. Stimulation occurred within a few minutes after addition of VBS. If the cells were incubated without substrate, VBS led to a loss of ATP. When the incubation buffer contained inosine, adenine and fumarate, loss of ATP was minimized (control,  $4.20 \pm 0.14$  mM; VBS,  $3.61 \pm 0.14$  mM). VBS-treated cells had a higher total sodium concentration than control cells. After 30 min. of incubation, cell sodium concentrations were  $7.09 \pm 0.49$  mM in the controls and  $11.30 \pm 0.92$  mM in VBS-treated cells. Incubation in a sodium-free medium reduced the cell sodium of VBS-treated cells to the concentration found in control cells incubated in regular buffer with 140 mM sodium. ATP concentrations were the same in control and VBS-treated cells incubated in sodium-free buffer. Since VBS-treated cells in sodium-free buffer had the same sodium and ATP concentrations as did control cells in regular buffer, but still had a doubled rate of 3-O-methylglucose entry, stimulation of transport is not likely to be due simply to ATP depletion. The mechanism of sugar transport stimulation may be related to increased carrier mobility induced by altered function of microtubular proteins. (Supported by USPHS 5 R01 HL 13029-05).

**TH-AM-G6 DIFFUSION OF PROTOPORPHYRIN INTO AND OUT OF ERYTHROCYTES IN VIVO: HUMAN**

**ERYTHROPOIETIC PROTOPORPHYRIA VS GRISEOFULVIN-INDUCED MURINE PROTOPORPHYRIA -A.A. Lamola**  
M.B. Poh-Fitzpatrick, F.H. Doleiden, G. Zalar and M. Weinstein, Bell Laboratories, Murray Hill, N.J. 07060 and Columbia University College of Physicians and Surgeons, New York 10032

It is expected that the site of excess protoporphyrin (PP) production in drug-induced protoporphyria, e.g., griseofulvin-induced murine protoporphyria (GFPP) is the liver<sup>1</sup>. It has been suggested that the erythropoietic system is the exclusive site of excess PP production in erythropoietic protoporphyria (EPP)<sup>2</sup>. However, examination of the distribution of PP in the following pools: feces, plasma, erythrocytes, erythrocyte membranes, and that bound to hemoglobin (Hb-PP), is virtually identical for GFPP and EPP. The two diseases are differentiated by the distribution of PP (which is chiefly Hb-PP) in erythrocytes of increasing age in circulation. We have previously shown<sup>2</sup> that PP rapidly leaks from circulating erythrocytes in EPP. We have now observed that the PP concentration increases with erythrocyte age in GFPP. From competition experiments we determined that the relative binding strengths of PP to erythrocyte membranes, plasma proteins (chiefly HSA) and Hb, normalized to concentrations found in the blood, are 1:2:240, respectively. We also found that the erythrocyte membrane provides only a small kinetic barrier to the transfer of PP from Hb to plasma sites and vice versa. Thus, the high erythrocyte PP levels found in GFPP is consistent with hepatic production, and the rapid leak of PP from EPP erythrocytes *in vivo* requires very efficient clearance of plasma-PP by the liver. Fluorescence microscopic examination of bone marrow specimens supports our model.

1. K. Nakao, et al., J. Lab. Clin. Med., 70, 923 (1967.)
2. S. Piomelli, et al., J. Clin. Invest. 56, 1519 (1975); A.A. Lamola et al., J. Clin. Invest. 56, 1528 (1975).

**TH-AM-G7 HEPATIC Na-K TRANSPORT IN CIRCULATORY SHOCK.** M.M. Sayeed, I.H. Chaudry, and A.E. Baue. Dept. Physiol., Loyola Univ. Sch. Med., Maywood, IL 60153 and Dept. Surg., Yale Univ. Sch. Med., New Haven, Ct. 06520

Cell failure and eventual cell death following decreased tissue perfusion is typical in irreversible circulatory shock. It has been suggested that alterations in membrane transport of electrolytes might play an important role in the pathogenesis of shock. We have studied hepatic Na-K transport to determine the relevance of alterations in this function in shock. Rats were subjected to shock by bleeding them to 50% of total blood volume. The ensuing hypotension ( $\approx 40$  mm Hg) was maintained for 1/2, 1 or 2 hours. Net Na and K movements were measured with chilling ( $0.5^\circ$  for 90 min) and rewarming ( $37^\circ$  for 60 min) of liver slices in an oxygenated Krebs-Ringer bicarbonate medium. The magnitude and direction of change in tissue and intracellular Na or K with chilling was about the same in control and shock animal liver slices. With rewarming net decrease in Na was 147.8 mmoles/(Kg dry wt X hr) in controls, 24.4 after 1/2 hr shock, and not demonstrable in animals after 1 or 2 hrs shock. Active K reaccumulation was 139.38 mmoles/(Kg dry wt X hr) in controls, 29.4 after 1/2 hr, 15.8 after 1 hr and 10.29 after 2 hrs of shock. Replenishment of animal's blood volume restored Na-K transport to near control level in 1/2 hr shock but not in animals after 1 hr shock. Whereas Na-K transport was abolished after 1 hr shock, protein synthesis was decreased only to about 50% of control level. Decrease in cellular protein synthesis was parallel to decrease in ATP formation by liver slices of animals in shock. However, decreased ATP formation could not completely account for the observed failure of Na-K transport in shock. Furthermore, estimates of membrane permeability to Na and K ( $P_{Na}/P_K$ ) could not provide evidence of overt membrane leaks. These data suggest that membrane bound Na-K transport mechanism is directly affected in shock.

**TH-AM-G8 TRANSIENT ACCUMULATION AND RELEASE OF CALCIUM BY SARCOPLASMIC RETICULUM VESICLES.** M. M. Sorenson\* and L. de Meis\* (Intr. by P.W. Brandt), Instituto de Biofisica, Universidade Federal do Rio de Janeiro, Brasil.

In the absence of oxalate, as much as 50% of the  $Ca^{++}$  initially accumulated by isolated sarcoplasmic reticulum vesicles may be released spontaneously over a period of several minutes. In the first two minutes, before  $Ca^{++}$  release begins, the ATP-dependent  $Ca^{++}$  accumulation can reach 200 to 250 nmoles/mg protein. The spontaneous release of the "extra"  $Ca^{++}$  initially accumulated appears to be triggered by the attainment of a sufficiently high concentration of free  $Ca^{++}$  inside the vesicles. After 5 to 7 minutes, net  $Ca^{++}$  loss ceases and  $Ca^{++}$  retention by the vesicles approaches a new, lower steady state. The amplitude of the transient phase of  $Ca^{++}$  accumulation reaches a high value near pH 6.0 and disappears above pH 6.5. In the presence of adequate substrate and external  $Ca^{++}$  ( $\geq 7 \mu M$ ), it is increased by free  $Mg^{++}$ . At optimal concentrations of  $H^+$  and  $Mg^{++}$ , the amount of  $Ca^{++}$  accumulated during the transient is augmented by various anions, in the order maleate  $\geq$  propionate  $\geq$  succinate  $>$  chloride  $>$  sulfate  $>$  acetylglycine. The divalent anions have their maximum effects at 20-40 mM and the monovalent anions, at 40-200 mM. At 200 mM, all of the carboxylic anions tested significantly reduce the amount of  $Ca^{++}$  retained in the steady state. Supported by Brazilian funds from CNPq, CEPEG, and BNDE (FUNTEC 241).

**TH-AM-G9 POTASSIUM PERMEABILITY OF CARDIAC MUSCLE IN TISSUE CULTURE.** C.R. Horres and M. Lieberman, Becton-Dickinson Research Center, Research Triangle Park, N.C. 27709 and Department of Physiology, Duke University Medical Center, Durham, N.C. 27710.

Potassium permeability of adult and embryonic cardiac muscle has generally been considered independent of the external potassium concentration,  $[K]_o$ , except at values below 2.5 mM (e.g. Carmeliet *et al.*, *J. Physiol (Lond)* 254:673, 1976). Growth oriented embryonic chick heart cells in tissue culture (Horres, Lieberman, *Circulation* 51 [Suppl. II]: 20, 1975) were studied with electrophysiological and  $^{42}K$  exchange techniques. When diffusional limitations are minimized, potassium permeability is relatively constant ( $\approx 5 \times 10^{-7} \text{ cm} \cdot \text{sec}^{-1}$ ) over the range of  $[K]_o$  from 1 to 20 mM. Mathematical simulations of tracer measurements indicate that diffusional limitations can produce an apparent decrease in potassium flux at low  $[K]_o$ . Experimental support for the predicted effect of radial diffusion on tracer exchange was obtained by comparing the rate of potassium loss in K-free solutions with preparations grown to about four times the average weight. In addition, when membrane potentials obtained in K-free solutions were correlated with  $^{42}K$  efflux measurements under the same conditions, the depolarization could be attributed to a loss of internal potassium rather than to a decrease in potassium permeability. These findings suggest that the effect of low  $[K]_o$  on membrane permeability in homeothermic cardiac muscle should be re-evaluated. Supported in part by grants from NIH (HL-12157), North Carolina Heart Assn. and Established Investigatorship from the American Heart Assn. to M.L.

**TH-AM-G10 EFFECT OF INSULIN UPON NA EFFLUX AS A FUNCTION OF INTRACELLULAR NA.** S.Y. Chan and R.D. Moore, Dept. Biology, S.U.N.Y., Plattsburgh, N.Y., 12901. (S.Y. Chan is presently at the Dept. Physiology, I.U.P.U.I. School of Medicine, Indianapolis, Ind.)

A kinetic analysis of the effect of insulin upon active Na efflux from frog skeletal muscle (Moore, 1973, J. Physiol. 232:23) indicated that the effect of insulin was due to an increase in the affinity of the carrier sites toward  $\text{Na}^+$ . If this hypothesis is correct, one would expect to see greater effects of insulin upon Na efflux from cells with low intracellular Na ( $\text{Na}_i$ ) than from cells with elevated  $\text{Na}_i$ . Accordingly, frog sartorius muscles were loaded to various levels of  $\text{Na}_i$ . In Ringer containing 104 mM  $\text{Na}^+$  and 10 mM  $\text{K}^+$ , the stimulation of  $^{22}\text{Na}$  efflux by insulin did decrease with increasing levels of  $\text{Na}_i$  ( $P < 0.005$ ); no effect was observed as  $\text{Na}_i$  reached 19 mM/Kg muscle wet weight as determined at the end of the experiment. When  $10^{-4}$  M ouabain was added to this Ringer, the same pattern was observed, the stimulation of  $^{22}\text{Na}$  efflux decreasing with increasing levels of  $\text{Na}_i$  ( $P < 0.005$ ). However, stimulation of  $^{22}\text{Na}$  efflux was still observed up to levels of  $\text{Na}_i$  approaching 55 mM/Kg. When the same type of experiment was conducted in K-free Ringer ( $\text{Na} = 114$  mM) containing  $10^{-4}$  M ouabain, the same decrease in stimulation with increasing levels of  $\text{Na}_i$  was observed ( $P < 0.005$ ), but the extrapolation of the curve of percent stimulation versus  $\text{Na}_i$  indicated that the effect would not have disappeared until levels of  $\text{Na}_i$  approached about 96 mM/Kg. In all three types of experiments, the percent stimulation was highest at normal levels of  $\text{Na}_i$  (about 7 mM Na/Kg), and the maximal percent stimulation obtained by extrapolation (to  $\text{Na}_i = 0$ ) was about 50%. As predicted, an inverse correlation exists between the stimulation by insulin of  $^{22}\text{Na}$  efflux and levels of  $\text{Na}_i$ .

**TH-AM-G11 EFFECT OF  $\text{NH}_4^+$  AND  $\text{HCO}_3^-/\text{CO}_2$  ON INTRACELLULAR  $\text{Cl}^-$  IN APLYSIA NEURONS.**

John M. Russell, Department of Physiology and Biophysics, University of Texas Medical Branch, Galveston, Texas 77550.

A relationship between intracellular pH ( $\text{pH}_i$ ) regulation and transmembrane  $\text{Cl}^-$  fluxes in squid axon has recently been shown (Russell and Boron, Nature, 263, 1976). The present study examines the effects of substances which are known to directly change  $\text{pH}_i$  on intracellular  $\text{Cl}^-$  levels. Intracellular  $\text{Cl}^-$  levels in giant Aplysia neurons were measured with liquid ion-exchanger  $\text{Cl}^-$ -selective microelectrodes. These electrodes had a 10 to 1 selectivity for  $\text{Cl}^-$  over  $\text{HCO}_3^-$ . Application of 50 mM  $\text{HCO}_3^-/5.4\%$   $\text{CO}_2$  for 30 min. caused a fall of internal  $\text{Cl}^-$  from 38.4 mM to 32.6 mM ( $n = 6$ ). On the other hand, 50 mM  $\text{NH}_4^+$  treatment for the same duration resulted in an increase of internal  $\text{Cl}^-$  from 36.2 mM to 40.7 mM ( $n = 5$ ). Upon return to control sea water, the internal chloride declined, usually below the control values, to an average of 32.7 mM. If instead of returning to control sea water, the  $\text{NH}_4^+$ -treated cell was washed with 50  $\text{HCO}_3^-/5.4\%$   $\text{CO}_2$  internal  $\text{Cl}^-$  declined even further, to an average of 28.4 mM ( $n = 4$ ). However, if during  $\text{NH}_4^+$ -treatment, 0.5 mM SITS (4-acetamido-4'-isothiocyanato-stilbene-2,2'-disulfonic acid) was applied, the effect of washing with 50  $\text{HCO}_3^-/5.4\%$   $\text{CO}_2$  was greatly reduced. In this case internal  $\text{Cl}^-$  activity fell from 37.2 mM to 35.7 mM ( $n = 3$ ). These results, in view of the already-reported effects of  $\text{NH}_4^+$  and  $\text{HCO}_3^-/\text{CO}_2$  on  $\text{pH}_i$  in squid axons (Boron and DeWeer, J. Gen. Physiol., 67: 91, 1976) and snail neurons (Thomas, J. Physiol., 238: 159, 1974) suggest that these net movements of  $\text{Cl}^-$  result from changes in  $\text{pH}_i$  and that these internal  $\text{Cl}^-$  changes are mediated by a system inhibited by the anion flux inhibitor, SITS. Thus, like in squid axon a  $\text{Cl}^-/\text{HCO}_3^-$  exchange system may play a role in  $\text{pH}_i$  regulation. Supported by NIH Grant NS-11946.

**TH-AM-G12 EFFECT OF EXTERNAL POTASSIUM IONS ON Na-Na AND Na-K EXCHANGES IN STRIATED MUSCLE.**

Brian G. Kennedy and Paul De Weer, Washington University School of Medicine, St. Louis, Missouri 63110.

Unidirectional influxes of  $^{22}\text{Na}$  and  $^{42}\text{K}$  were measured in *Rana pipiens* sartorius muscles whose Na levels had been elevated, and K levels depleted, by 24 hours storage at 3°C. Exposure to 0.38 mM dinitrofluorobenzene (DNFB) for 30 minutes has been shown (J. Gen. Physiol. 68: 405; 1976) to raise internal ADP, to lower ATP, and to stimulate sodium pump mediated Na-Na exchange. We now report on the relationship between Na-Na exchange and Na-K exchange, specifically on the question whether Na-Na exchange, induced by metabolic poisoning, supplants, or occurs in addition to, normal Na-K exchange. Influx of  $^{22}\text{Na}$  was determined in control and DNFB treated muscles at 0, 2.5, 5 and 10 mM external K. In DNFB muscles, strophanthidin sensitive unidirectional sodium influx (a measure of sodium pump mediated Na-Na exchange) decreased from 15  $\mu\text{mol/g.h}$  in 0 mM K Ringer's solution to negligible levels in 10 mM K Ringer's. There was little strophanthidin sensitive Na influx in control muscles not exposed to DNFB. This inhibition, by external K, of sodium pump mediated Na influx may be viewed as a counterpart to the inhibition of sodium pump mediated K influx by external Na, shown by Sjödin and Medici (Nature 255: 632, 1975). Comparisons were made between the stimulatory effect of external K on strophanthidin-sensitive K influx in normal and DNFB treated muscles, and also between the stimulatory effect of K on pump-mediated K influx, and the inhibitory effect of K on pump-mediated Na influx, both in DNFB-poisoned muscles. Supported by funds from the Muscular Dystrophy Association.

**TH-AM-G13 PUMP-MEDIATED Na-Na EXCHANGE IN INTERNALLY DIALYZED SQUID GIANT AXONS.****Paul De Weer.** Washington University School of Medicine, St. Louis, Missouri 63110.

The sodium pump of squid giant axon, human erythrocytes, and frog skeletal muscle is capable of catalyzing Na-Na exchange as well as the usual Na-K exchange. Pump-mediated Na-Na exchange takes place to a sizeable extent only when intracellular ADP levels are elevated. It has not been resolved whether, for a given ATP level, ADP-induced Na-Na exchange occurs exclusively in addition to, or partly substitutes for, pre-existing Na-K exchange. The answer to such kinetic questions can only be obtained from preparations such as these internally dialyzed squid giant axon, where intra- as well as extracellular fluid composition can be controlled during isotopic flux experiments. The present experiments establish that the sodium pump of internally dialyzed squid giant axons can be made to engage in Na-Na exchange, and pave the way for a more detailed investigation of the kinetics of Na-K and Na-Na exchange as a function of intracellular nucleotide composition. Axons were internally dialyzed with solutions where the ATP/ADP ratio was either kept high by means of phosphoenolpyruvate, via the pyruvate kinase reaction, or maintained at a low value by means of L-arginine, via the arginine phosphokinase reaction. Efflux of  $^{22}\text{Na}$ , at high ATP/ADP ratios, was stimulated by external K and inhibited by external Na; at low ATP/ADP ratios, it was little affected by K but stimulated by external Na. Low ATP/ADP ratios also induced the appearance of a strophanthidin-sensitive sodium influx; this sodium influx could be inhibited by raising extracellular K. Supported by NIH grant NS 11223.

**TH-AM-G14 THE CONTROL OF IONIZED CALCIUM IN SQUID AXONS.** J. Requena, R. DiPolo, F. J. Brinley, Jr. and L. J. Mullins, Centro de Biofísica y Bioquímica, IVIC, Caracas, Venezuela; Department of Physiology and Department of Biophysics, University of Maryland School of Medicine, Baltimore, Md. 21201.

Measurement of the Ca content of squid axoplasm by atomic absorption shows a value of  $60 \mu\text{mol/kg}$  for fresh axons. This value does not change with time if axons are stored in 3 mM Ca (Na) seawater. In 10 mM Ca (Na) seawater, it increases with time, while in choline seawater the Ca content of axoplasm increases at 10-50 times the rate in 10 mM Ca (Na) seawater. If the Na concentration of seawater is decreased from 450 to 180 mM, the ionized Ca concentration as judged by light emission from aequorin confined to a dialysis capillary at the center of the axon is unchanged. Na concentrations in seawater of 90 or 45 mM lead to substantial increases in ionized Ca in axoplasm. In axons preinjected with apyrase so that their ATP concentration is very low, the level of ionized Ca is the same as in control axons over many hours. If ionized Ca is deliberately raised either by increasing  $\text{Ca}_o$  or decreasing  $\text{Na}_o$ , recovery to normal values of Ca, ensues promptly upon the application of 3 mM Ca (Na) seawater. Depolarization of axons by the application of 100 mM K seawater leads to about a 5-fold increase in internal ionized Ca concentration; the application of normal seawater reverses this change. The application of 2 mM CN seawater to a freshly isolated squid axon leads to an increase in internal ionized Ca concentration to only double its initial value, with a delay of 2-4 hr; a similar result is obtained if FCCP is used as an inhibitor except that the Ca release is virtually without delay. In an apyrase-injected axon, the effect of CN in releasing Ca from internal stores is also virtually without delay. We conclude that the maintenance of a normal  $[\text{Ca}]_i$  is dependent on  $[\text{Na}]_o$ ,  $E_m$  and  $[\text{Ca}]_o$ . [Aided by grants from NINDS (NS05846, NS13420) and NSF (GB41593)]

**TH-AM-G15 CALCIUM-DEPENDENT SODIUM EFFLUX IN MYXICOLA GIANT AXONS.** R. F. Abercrombie and R. A. Sjödin. Department of Biophysics, University of Maryland School of Medicine, Baltimore, Maryland 21201.

Giant axons from the marine annelid *Myxicola infundibulum* were microinjected with  $^{22}\text{Na}$  and the dependence of Na efflux on  $[\text{Ca}]_o$  was studied. In axons with normal  $[\text{Na}]_i$  (15-25 mM/kg), no change in Na efflux occurred upon removal of Ca from either Na or Li seawater in the presence of  $10^{-4}$  M ouabain. When  $[\text{Na}]_i$  was elevated to about 90 mM/kg by microinjection of unlabelled Na in addition to  $^{22}\text{Na}$ , removal of  $\text{Ca}_o$  from 10 mM Ca-Li seawater in the presence of ouabain brought about a reversible reduction in Na efflux amounting to one-third of the Na efflux in the 10 mM Ca-Li-ouabain solution. Similar experiments performed in Na seawater revealed no change in Na efflux upon removal of  $\text{Ca}_o$ . However, when  $[\text{Ca}]_o$  was elevated to values above 10 mM in Na seawater containing  $10^{-4}$  M ouabain, a  $\text{Ca}_o$ -free effect was observed in Na seawater as well. It is concluded that *Myxicola* giant axons show a  $\text{Ca}_o$ -dependent Na efflux. The properties deduced thus far for this component of Na efflux in *Myxicola* are: 1) Activation by  $\text{Ca}_o$ ; 2) Activation by  $\text{Na}_i$ ; 3) Competitive inhibition by  $\text{Na}_o$ ; and 4) Insensitivity to ouabain.

(Supported by grants from NIH (NS07626) and NSF (BMS 74-12343))